Journal of Physiology (2002), **540.2**, *pp.* 509–527
DOI: 10.1113/jphysiol.2001.013441

www.jphysiol.org

A fundamental oscillatory state of isolated rodent hippocampus

Chiping Wu *‡, Hui Shen *, Wah Ping Luk * and Liang Zhang *†‡

* *Toronto Western Research Institute, University Health Network,* † *Department of Medicine* (*Division of Neurology*)*and* ‡ *Bloorview Epilepsy Research Program, University of Toronto, Toronto, Ontario, Canada, M5T 2S8*

Population neuronal rhythms of various frequencies are observed in the rodent hippocampus during distinct behavioural states. However, the question of whether the hippocampus exhibits properties of spontaneous rhythms and population synchrony in isolation has not been definitively answered. To address this, we developed a novel preparation for studying neuronal rhythms in a relatively large hippocampal tissue *in vitro*. We isolated the whole hippocampus from mice up to 28 days postnatal age, removing the dentate gyrus while preserving the functional CA3-to-CA1 connections. Placing the hippocampal isolate in a perfusion chamber for electrophysiological assessment extracellular recordings from the CA1 revealed rhythmic field potential of 0.5 to ⩽ 4 Hz that occurred spontaneously and propagated along the ventro–dorsal hippocampal axis. We provide convergent evidence, via measurements of extracellular pH and K^+, recordings of synaptic and intracellular activities and morphological assessments, verifying that these rhythms were not the consequence of hypoxia. Data obtained via simultaneous extracellular and patch clamp recordings suggest that the spontaneous rhythms represent a summation of GABAergic IPSPs originating from pyramidal neurons, which result from synchronous discharges of GABAergic inhibitory interneurons. Similar spontaneous field rhythms were also observed in the hippocampal isolate prepared from young gerbils and rats. Based on these data, we postulate that the spontaneous rhythms represent a fundamental oscillatory state of the hippocampal circuitry isolated from extra-hippocampal inputs.

(Received 24 October 2001; accepted after revision 17 January 2002)
Corresponding author L. Zhang: Mclaughlin Pavilion, Room 13-411, Toronto Western Hospital, 399 Bathurst Street, Toronto, Ontario, Canada M5T 2S8. Email: liangz@uhnres.utoronto.ca

In the hippocampus synchronous population neuronal activity of various frequencies are observed during distinct behavioural states. Hippocampal EEGs of freely moving animals exhibit three main components: large amplitude irregular activity (LIA, 0.5–20 Hz), rhythmic slow activity (RSA or θ, 4–10 Hz) and fast oscillatory activity (γ, 30–100 Hz). Primarily, LIA occurs during slow-wave sleep and in-wake immobility, whereas RSA and γ rhythms are associated with exploration and rapid-eye movement sleep (Stumpf, 1965; Vanderwolf, 1969; Bland *et al.* 1975; Buzsáki *et al.* 1983; Leung *et al.* 1985; 1998). While the genesis and function of these hippocampal rhythms have not been fully elucidated, numerous studies suggest that they play important roles in synaptic plasticity (Huerta & Lisman, 1993), sensory-motor behaviour (Oddie & Bland, 1998) and learning and memory processing (Winson, 1978; Buzsáki, 1989; Wilson & McNaughton, 1994; Kudrimoti *et al.* 1999; Tesche & Karhu, 1999 or 2000).

In the past two decades, numerous studies using the hippocampal slice preparation have tried to address the cellular mechanisms of rhythm generation. It has been increasingly recognized that the local circuit of slices contains necessary structures to oscillate following pharmacological manipulation or repetitive afferent stimulation. Induction of various rhythmic activities has been reported in the slice, including those in the δ (0.5 to ⩽ 4 Hz, Zhang *et al.* 1998; Fellous & Sejnowski, 2000), θ (4–10 Hz, Konopacki *et al.* 1987; MacVicar & Tse, 1989; Williams & Kauer, 1997; Chapman & Lacaille 1999) or γ (Whittington *et al.* 1995; Fisahn *et al.* 1998; Bracci *et al.* 1999) band. The use of the hippocampal slice as a convenient *in vitro* model system (Lynch & Schubert, 1980) has given us numerous insights into the cellular basis of hippocampal rhythmicity. However, it possesses an inherent limitation – many long-range neuronal connections are removed by the slicing procedure and spontaneous population oscillations characteristic of hippocampal EEG activity seen *in vivo* do not occur in the conventional rodent hippocampal slices.

Over the past few years evidence has been gathering to indicate that the hippocampus exhibits extensive neuronal connections that extend well beyond the boundaries of

C. P. Wu and H. Shen contributed equally to this work.

thin conventional transverse slices. Using anterograde tracing or combined intracellular recording–labelling techniques in intact rats, Ishizuka *et al.* (1990) and Li *et al.* (1994) have shown that the axon projections to the CA1 from CA3 pyramidal neurons distribute to about two-thirds (a few millimetres) of the ventro–dorsal axis of the hippocampus. The projections forming the perforant pathway from the entorhinal cortex to the dentate gyrus also exhibit extensive divergent spread (Dolorfo *et al.* 1998). Aside from excitatory connections, GABAergic inhibitory interneurons (INs) also possess extensive axon–dendrite arbors (see review by Freund & Buzsáki, 1996), and networks of horizontally orientated INs can extend up to several millimetres along the ventro–dorsal axis of the rat hippocampus (Gulyás *et al.* 1996; Fukuda & Kosaka, 2000). Such divergent hippocampal network connectivity has been the focus of several recent studies, demonstrating its significance in basic hippocampal physiology (Andersen *et al.* 2000) and information processing related to spatial learning and memory (Moser & Moser, 1998; Hampson *et al.* 1999). We hypothesize that divergent network connectivity functions to integrate and synchronize spatially distributed neurons. If this is true it would therefore be important for the generation of population synchrony and oscillations in the hippocampus. We thus re-examined the question put forth by Bland and Colom in their 1993 review of hippocampal oscillations: does the hippocampus exhibit properties of oscillation and synchrony in isolation, and if so what are the underlying cellular and network mechanisms?

Khalilov *et al.* (1997) recently described a novel model system that greatly motivates the *in vitro* investigation of hippocampal network activity. By isolating an *in vitro* perfusion of the whole neonatal rat hippocampus, their model permits electrophysiological assessment of the hippocampus at both single cell and network levels. However, in Khalilov's study their animals were limited to <10 days old because hippocampi isolated from more developed rats did not survive *in vitro* probably due to insufficient oxygenation of the thicker tissue (Khalilov *et al.* 1997). As in rodents dramatic developmental changes in hippocampal neurons occurs during the second postnatal week, stabilizing to near-mature levels after the third postnatal week, as defined via their morphological and electrophysiological properties (Zhang *et al.* 1991; Spigelman *et al.* 1992; Ben-Ari *et al.* 1997; Gomez-Di Cesare *et al.* 1997). We decided to modify Khalilov's approach in an attempt to study network activity in the more mature rodent hippocampus.

For this undertaking we developed a tissue isolation and perfusion system based upon the report by Khalilov *et al.* (1997). Our system allows the isolation of the hippocampal tissue from mice up to 28 days old while preserving the functional integrity of the extensive CA3-to-CA1 connections *in vitro*. As hypothesized, rhythmic field potentials of 0.5 to $\leqslant 4$ Hz were found to occur spontaneously and propagate throughout the mouse hippocampal isolate. Some of the present data have been presented in abstract form (Wu *et al.* 1999; Luk *et al.* 2000; Shen *et al.* 2000).

METHODS

Preparations of the hippocampal isolate

Mice (C57Bl), 21–28 days old (Charles River, Quebec, Canada) were used in the present experiments. All experiments were carried out according to the Canadian Animal Care Guidelines and approved by the animal care committee of our institution. The procedure of tissue isolation was similar to that described by Khalilov *et al.* (1997). Briefly, after decapitation under halothane anaesthesia, the brain was quickly removed and maintained in an ice-cold artificial cerebrospinal fluid (ACSF). The hippocampus was then dissected out from the hemi-sectioned brain and the dentate gyrus area beyond hippocampal fissure was removed. By doing so, we obtained a relatively flat tissue of ~0.6 mm thickness that included CA1, CA2 and CA3b and c areas. The tissue dissection was carried out in the oxygenated, ice-cold ACSF using fine paint brushes and custom made micro-glass probes, visualized under a dissecting microscope. After dissection, the hippocampal isolate was maintained in the oxygenated ACSF at room temperature (21–22°C) for at least 1 h before transferring to the recording chamber. The components of the ASCF were (mM): 3.5 KCl, 1.25 NaH_2PO_4, 125 NaCl, 25 $NaHCO_3$, 2 $CaCl_2$, 1.3 $MgSO_4$ and 10 glucose, with pH ~7.4 when aerated with 95 % O_2–5 % CO_2. In some experiments, aided by a dissecting microscope, we made additional transverse or longitudinal cuts of the hippocampal isolate (see Figs 9 and 10).

Perfusion apparatus

We used a submerged recording chamber of inner dimensions 3.5 × 5 × 20 mm (depth × width × length). Viewing was assisted via a dissecting microscope and a fibre-optic light source. The hippocampal isolate was held on a stainless steel fine mesh (0.015 inch grid length) via an imbedded array of six to eight mosquito pins. We set the mesh approximately 1.5 mm above the bottom of the chamber to allow the perfusion of the oxygenated ACSF to both sides of the isolated tissue. The perfusate was maintained at 31–32°C by an automatic system. The water bath underneath the recording chamber was also set at 32°C via an automatic temperature control unit, to provide warm, humidified 95 % O_2–5 % CO_2 passing over the perfusate. In our experimental setting we found that it was critical to perfuse the hippocampal isolate with a high flow rate (~15 ml min^{-1}) but at minimally submerged levels. This was because excessive accumulation of the perfusate over the hippocampal isolate caused a time-dependent deterioration of the evoked and spontaneous synaptic field responses. We suspect that the accumulation of the ACSF over the perfused tissue, as occurs in recording settings that use a water-immersed lens for viewing, may cause inadequate perfusion of the hippocampal isolate thus leading to hypoxic suppression of synaptic activity.

Electrophysiological recordings

Glass pipettes filled with 150 mM NaCl (resistance of 1–2 MΩ) were used for extracellular recordings. To avoid pushing the electrode through the dense layer of alveus axons, we placed the hippocampal isolate in the recording chamber with its stratum

radiatum side facing up and positioned the electrode at an angle of ~70 deg with respect to the horizontal plane. Field potentials were sampled through an Axoclamp-2A or 2B amplifier (Axon Instruments Inc., Union City, CA, USA). Due to the small amplitudes of spontaneous field rhythms (30–300 μV), these responses were further amplified to a total gain of × 10 000 before digitization. The bandwidth of the Axoclamp amplifier was set in the range of 0–300 Hz to reduce high frequency noise. We found that removing high frequency signals caused no substantial alteration in the waveform of the rhythmic field potentials. In some experiments we set the bandwidth of the Axoclamp amplifier in the range of 0–1 kHz to ensure the reliable recording of fast oscillatory responses. To stimulate the Schaffer collateral pathway, a bipolar tungsten electrode (50 μm in diameter) was placed into the CA2 region, and constant current pulses of 0.1–0.2 ms were generated by a Grass stimulator and delivered via an isolation unit. The bandwidth of the Axoclamp amplifier was set in the range of 0–3 kHz to sample evoked synaptic field potentials.

Whole-cell patch recording of individual neurons was conducted via a 'blind' approach method (Zhang *et al.* 1991, 1994, 1998). The components of the patch pipette (intracellular) solution were: 120 mM potassium gluconate, 2 mM Hepes, 0.1 mM EGTA and 0.5 % neurobiotin (pH 7.25 and 280–290 mosmol l^{-1}. The resistance of the patch pipettes was 4–5 MΩ when filled with this solution. We used a patch pipette with a relatively high tip resistance to reduce 'rundown' effects of whole-cell dialysis. In some experiments, IN responses were monitored in the cell-attached configuration (Verheugen *et al.* 1999). For perforated patch recordings, the patch pipette solution contained 150 mM KCl, 2 mM Hepes, 0.1 mM EGTA and gramicidin (⩽ 50 μg ml^{-1}, Sigma; Rhee *et al.* 1994). Intracellular responses were collected for analysis only if the access resistance of the perforated configuration was ⩽ 80 MΩ (Zhang *et al.* 1996). Voltage- and current-clamp recordings were conducted via an Axopatch-200B or Axoclamp-2B amplifier (Axon Instruments). Data acquisition, storage and analyses were done via using pCLAMP software (version 8, Axon Instruments). Digitization was via a 12-bit D/A interface (Digidata 1200, Axon Instruments).

Measurements of basic intracellular parameters have been described previously (Zhang *et al.* 1991, 1994, 1998). The phase relation between the field rhythms and intracellular responses of individual neurons was analysed from a stable recording period of ⩾ 60 s. Briefly, we measured the period of the rhythmic field potential (T) and the time interval between correlated extracellular and intracellular responses (t). The timing of the peak response was measured because it was often difficult to determine the baseline. The phase shift of intracellular synaptic responses *vs.* the field rhythms was calculated by the formula: $(t \times 360)/T$, taking the peak of rhythmic field potentials as reference (zero phase shift, Koch & Segev, 1992). Power spectrum and cross correlation plots were generated via using Micro-Origin software (version 6). Statistical significance was determined using Student's t test or one-way ANOVA (Micro-Origin).

Measurements with K^+- and pH-sensitive electrodes

Ion-sensitive glass electrodes were prepared as per Ammann (1986), Morris (1995) and Amzica & Steriade (2000). These glass electrodes were acid cleaned, dried, exposed briefly to dimethyldichlorosylane vapour (14896, Fluka) and then baked at 120°C for several hours. The tip diameter of these electrodes was ~20 μm. For making the K^+ electrodes, one barrel of the two-barrel electrode was filled at the tip with potassium ionophore-I cocktail A (Fluka, Buchs, Switzerland) and then back-filled with 200 mM KCl, and the reference barrel was filled with 200 mM NaCl. For the pH electrode, the sensing barrel was filled with hydrogen ionophore-II cocktail A (Fluka, Buchs, Switzerland) and then back-filled with a solution containing 100 mM NaCl, 20 mM Hepes and 10 mM NaOH (pH 7.25). These ion-sensitive electrodes were inserted into the centre of the hippocampal isolate (200–300 μm in depth) to monitor ionic activity of the extracellular space. Signals were recorded using a differential, high impedance ion-sensitive electrode amplifier ($> 10^{14}$ Ω, AM Systems, Carlsborg, WA, USA). K^+ and H^+ calibration solutions were similar to the ACSF with either KCl or $NaHCO_3$ substituted for corresponding molecules of NaCl. The sensitivity of the K^+- or pH-electrode was 62.5 ± 1.9 mV for an increase of K^+ concentrations from 3.5 to 35 mM (n = 11) or 50.8 ± 0.4 mV for a change in pH from 6.8 to 7.8 (n = 9). The ion-sensitive electrodes were calibrated before and after the intratissue measurement, and the measurements were included for data analysis if stable calibration responses were achieved.

Morphological assessments

After maintenance in ACFS at 31–32°C for about 4 h, the hippocampal isolate was fixed in 4 % paraformaldehyde/0.1 M phosphate buffer. Paraffin-embedded sections of 6 μm thick were cut along the transverse plane of the hippocampus and stained with cresyl violet (Shinno *et al.* 1997). Staining neurobiotin-filled neurons was performed as previously described (Zhang *et al.* 1998). After termination of the whole-cell recording, hippocampal isolate was fixed with 4 % paraformaldehyde/0.1 M phosphate buffer and vibratome sections of 100 μm thickness were obtained along the horizontal plan of the hippocampal isolate. Fixed sections were exposed to a biotin–avidin complex, rinsed and reacted with diaminobenzidine (DAB) and H_2O_2 (ABC kit, Vector Laboratory). The tissue sections were viewed and photographed under a Nikon light microscope (Optiphot), and a Zeiss camera lucida drawing device was used to trace the neurobiotin-stained cellular processes.

Identification of individually recorded hippocampal neurons

CA1 pyramidal neurons and interneurons (INs) were recognized by their morphological and electrophysiological properties. In general, CA1 pyramidal neurons exhibited more negative resting membrane potentials and lower input resistance than INs (see Results). They barely fired from the resting membrane potentials, but discharged regularly with evident spiking adaptation as stimulated by intracellular injection of depolarizing current pulses (Zhang *et al.* 1994). In the fixed hippocampal isolate, the cell bodies of CA1 pyramidal neurons were found in horizontal sections ~200 μm (stratum pyramidale) below the hippocampal temporal surface, and the axons of CA1 pyramidal neurons ramified in temporal surface sections (alveus). Dendrites of CA1 pyramidal neurons could be seen in several sections made from stratum radiatum, with numerous spines on dendritic processes. In contrast to pyramidal neurons, INs often fired from tresting potentials, and when stimulated by intracellular injection of depolarizing current pulses, INs discharged in high frequencies with little firing adaptation. Morphologically, the cell bodies of INs were found in various CA1 sub-fields including oriens/alveus, stratum pyramidale or stratum radiatum (Freund & Buzsáki 1996; Lacaille *et al.* 1987; Parra *et al.* 1998).

Chemicals and pharmacological agents

All external and patch pipette solutions were made with de-ionized distilled water (specific resistance 18 MΩ cm^{-1}, Milli-Q system, Molsheim, France). Chemicals for making the patch-

pipette solution were purchased from Fluka (New York, USA). TTX, transmitter receptor agonists and antagonists were obtained from Tocris and RBI (Ontario, Canada).

RESULTS

General properties of spontaneous field rhythms

C57Bl mice of postnatal 21–28 days old were used in the present experiments except where indicated. After decapitation, we dissected out the whole hippocampus from the brain, and then removed the dentate gyrus area but preserved the CA3-to-CA1 connections. The hippocampal isolate was perfused in a submerged recording chamber and the perfusate temperature was kept at 31–32°C. Extracellular recordings from the CA1 revealed spontaneously occurring rhythmic potentials with amplitudes of 30–300 μV and a duration of 0.3–0.6 s. These rhythms could persist for up to 8 h under our recording conditions. Although the frequency and amplitude of these rhythms were stable in the first 4 h (Fig. 1) a trend of decline in the frequency of the rhythms was noted after *in vitro* perfusion for $\geqslant$ 5 h. Measured after 1–2 h of perfusion in the recording chamber the frequency of the CA1 spontaneous field rhythms was 1.4 ± 0.1 Hz (means ± S.E.M., n = 187 isolated hippocampal tissues). At higher recording temperatures, 35–36 °C, the CA1 field rhythms were slightly faster, 1.72 ± 0.23 Hz (n = 6), but still remained in range of the EEG delta band.

The waveform polarity of the CA1 field rhythms varied depending upon the position of the extracellular recording electrode. In general, negative (downward) waveform responses appeared in the recordings made from the dendritic areas of CA1 pyramidal neurons (stratum radiatum) where stimulation of the Schaffer collateral pathway induced typical field excitatory postsynaptic potentials (EPSPs; Fig. 1*C*). CA1 field rhythms with positive (upward) waveforms became prominent as the recording site moved towards the somatic area of CA1 pyramidal neurons (stratum pyramidale) as indicated by the appearance of somatic field potentials and large-amplitude population spikes following the afferent stimulation (Andersen *et al.* 1971; Lynch & Schubert, 1980; Fig. 1*B* in this paper). These observations were in keeping with the depth profile of the hippocampal RSA observed *in vivo* (Vanderwolf 1969; Buzsáki *et al.* 1983), however, a more detailed analysis is needed to characterize the sink–source relation of the *in vitro* slow rhythm.

To determine the synaptic nature of the spontaneous field rhythms, we perfused the hippocampal isolate with a modified ACSF in which Mg^{2+} was raised from 1.3 to 5 mM while the rest of the ACSF components were kept constant. Our previous experiments in rat hippocampal slices have shown that similar high Mg^{2+} treatment is sufficient to suppress evoked synaptic transmission in the CA1, presumably via attenuation of the spike-dependent Ca^{2+} entry in the pre-synaptic terminals (Ouanounou *et al.* 1999). In keeping with our previous observations, perfusion of the mouse hippocampal isolate with high Mg^{2+} ACSF caused a reversible blockade of the evoked field EPSPs in the CA1 as well as a suppression of the spontaneous field rhythms (n = 5, Fig. 1*B*). A blockade of CA1 field rhythms was also observed after adding 0.5 μM TTX into the standard ACSF (n = 3). Perfusion of the hippocampal isolate with the AMPA glutamate receptor antagonist CNQX at low concentrations (1–2 μM) suppressed the spontaneous field rhythms and reduced the amplitude of the evoked CA1 field EPSPs (n = 5, Fig. 1*C*). In contrast, a similar application of the NMDA receptor antagonist AP-5, at a concentration sufficient to block NMDA channel activity (50 μM, n = 4), failed to do so. Collectively, these observations indicate that the spontaneous field rhythms observed from the mouse hippocampal isolate are of synaptic origin, and their manifestation is dependent upon excitatory drive mediated by glutamatergic AMPA synapses.

Spontaneous rhythmic field rhythms were also found in the hippocampal isolate obtained from Mongolian gerbils (body weight $\leqslant$ 40 g, n = 5) and Wistar rats (12–14 days old, n = 6), with the frequencies of 2.13 ± 0.3 and 1.9 ± 0.16 Hz, respectively, as measured from the CA1. These rhythmic responses were abolished by high Mg^{2+} ACSF and 2 μM CNQX. Similar to the effects observed from the mouse hippocampal isolate (see below), perfusion of the gerbil or rat hippocampal isolate (n = 2 each) with the $GABA_A$ receptor antagonist bicuculline methiodide (5 μM) reversibly abolished the spontaneous field rhythms. Collectively, these pharmacological properties were similar to those we observed from the mouse hippocampal isolate. Thus, although the cellular mechanisms of these rhythmic activities in the gerbil or rat hippocampal isolate remains to be further characterized, the ability to generate spontaneous slow population rhythms appears to be a general phenomenon of the hippocampal isolate across rodent species.

Sanchez-Vives & McCormick (2000) have reported spontaneous rhythmic activities of ~2 Hz that occur in pyramidal neurons of ferret cortical slices as they were perfused in ACSF containing 3.5 mM K^+ and 1 mM each of Mg^{2+} and Ca^{2+}. To explore whether a similar ionic condition allows spontaneous rhythm to occur in local hippocampal circuitry, we prepared transverse slices (600 μm in thickness) from the ventral hippocampus of 27–28-day-old mice and perfused these slices with a similar ACSF as per Sanchez-Vives & McCormick (2000). In eight of the eight slices examined at 32 °C, extracellular recordings revealed no spontaneous rhythmic potentials in the CA3 and other hippocampal regions. However, bursting field responses of 0.5–2 mV and 0.03–0.1 Hz could be induced in these slices by adding 50 μM 4-aminopyridine (4-AP) into the perfusate, in keeping with the previous study in

rat hippocampal slices (Avoli *et al.* 1996). Thus, the spontaneous field rhythms we observed from the mouse hippocampal isolate appears not to be mimicked in the conventional hippocampal slices by using the perfusate with relatively low concentrations of Mg^{2+} and Ca^{2+}.

Controls for hypoxic influences

As emphasized in Khalilov's study (1997) a major concern of using the isolated hippocampal preparation *in vitro* is hypoxic influence. Our previous studies in rat hippocampal slices have shown that synaptic field potentials evoked from the CA1 are highly vulnerable to hypoxia and are readily abolished by brief hypoxic episodes (Zhang & Krnjević 1993; Perez-Velazques & Zhang 1994; Chung *et al.* 1998; Ouanounou *et al.* 1999). We therefore monitored these responses in the mouse hippocampal isolate as one of our controls. As shown in Fig. 2*A*, the CA1 field EPSPs remained at a stable level for several hours in response to constant stimulation of the Schaffer collateral pathway, arguing against the deteriorating effects of hypoxia on the CA1 glutamate synapses. The amplitudes of CA1 field EPSPs and somatic population spikes were 2.5 ± 0.1 mV (n = 112) and 4.8 ± 0.4 mV (n = 43), respectively, and the paired-pulse enhancement of the CA1 field EPSPs was 133.6 ± 2.3 % (inter-pulse interval = 50 ms). These measurements were compatible with those previously collected from rat hippocampal slices (see references above), suggesting that the afferent stimulation is capable of activating functional glutamatergic synapses in the mouse hippocampal isolate.

We next examined the activity of individual CA1 neurons in the hippocampal isolate using the whole-cell patch clamp recording technique. The recorded neurons were filled with neurobiotin during whole-cell dialysis, and

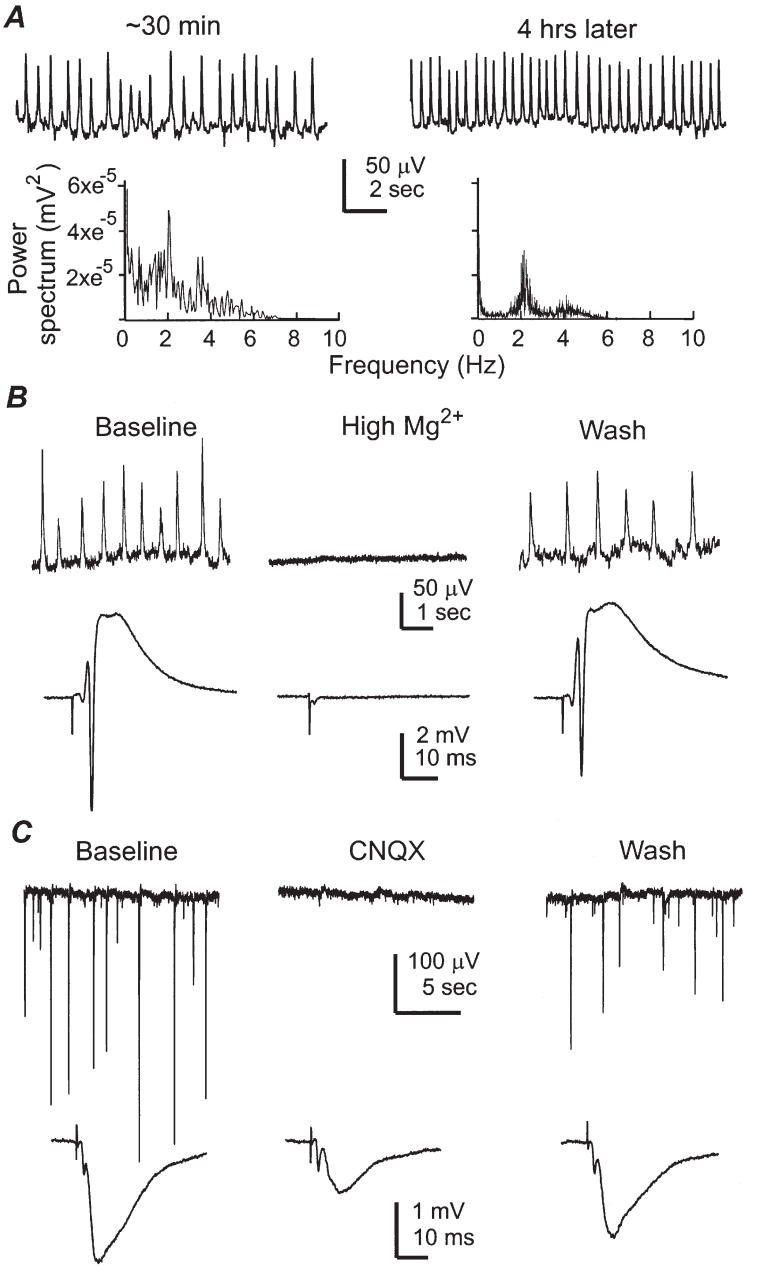

Figure 1. Spontaneous rhythms of synaptic origin

Data in *A–C* were collected from three separate experiments. *A*, rhythmic field potentials sampled from CA1 somatic area of a 25-day-old mouse hippocampal isolate. Left and right, responses collected at ~30 min after placing the tissue isolate in the recording chamber and ~4 h later, respectively. The corresponding power spectrum plots were shown below. In a set of five hippocampal tissues examined, the rhythms were 2.38 ± 0.15 and 2.04 ± 0.25 Hz measured after perfusion (at 32°C) for ~30 min and 4 h. *B*, spontaneous rhythmic field potentials (top) and evoked synaptic field potential (bottom) sampled from the CA1 somatic area of a 26 days old mouse hippocampal isolate. Representative responses were collected before, during perfusion of a high Mg^{2+} ACSF (5 mM, ~7 min) and after washing out high Mg^{2+}. The evoked potentials were induced by constant Schaffer collateral stimulation every 15 s and each illustrated trace was an average from three consecutive responses. *C*, spontaneous rhythmic field potentials (top) and evoked field EPSPs (bottom) were recorded from the CA1 dendritic area of a 28 days old mouse hippocampal isolate. Representative responses were collected before, at the end of CNQX perfusion (1 μM, ~8 min) and after washing out CNQX. The evoked responses were similarly illustrated as in *B*.

their morphology was examined after fixation and re-sectioning of the hippocampal isolate. Basic intracellular parameters measured from CA1 pyramidal neurons were: resting membrane potential −61.4 ± 0.6 mV, input resistance 117.1 ± 7.3 MΩ and action potential amplitude 112.4 ± 2.9 mV ($n = 54$). The intracellular parameters measured from inhibitory INs were: resting membrane potential −53.2 ± 1.1 mV, input resistance 152.0 ± 11.9 MΩ and action potential amplitude 88.5 ± 3.6 mV ($n = 36$). The parameters measured from CA1 pyramidal neurons of the mouse hippocampal isolate were not significantly different ($P \geqslant 0.4$, unpaired t test) from those collected from hippocampal slices of C57BL mice (resting potential −61.6 ± 2.6 mV, input resistance 107.2 ± 13.5 MΩ and action potential amplitude 115.3 ± 5.7 mV, $n = 9$ CA1 pyramidal neurons). Our data were also compatible with the intracellular study by Shuttleworth & Connor (2001) in mouse hippocampal slices.

We also examined the effect of baclofen, a $GABA_B$ receptor agonist, in attempting to control possible hypoxic interruption of the G protein-coupled signal cascades (Tanabe *et al.* 1998). Exposure of the hippocampal isolate to 50 μM baclofen induced a negative shift in the membrane potential (7.4 ± 0.8 mV, $n = 4$ CA1 pyramidal neurons) and reversibly abolished the spontaneous CA1 field rhythms in all hippocampal tissues examined ($n = 6$). These effects of baclofen were in agreement with the known actions of the pre- and post-synaptic $GABA_B$ receptors (Andrade *et al.* 1986; Scanziani *et al.* 1992). The observations, taken together with our finding of muscarinic θ oscillations as presented in a later section, indicate that G protein-coupled, receptor-mediated signal cascades function well in the mouse hippocampal isolate under our recording conditions.

To assess the ionic homeostasis of the hippocampal isolate directly, we measured extracellular pH and K^+ activity using ion-sensitive electrodes following protocols of Morris (1995), Ammann (1986) and Amzica & Steriade (2000). Extracellular pH, as sampled from the centre of the hippocampal isolate (200–300 μm in depth) was in the range previously measured from rat hippocampal slices, 7.15 ± 0.03 ($n = 9$) (Voipio & Kaila, 1993; Chesler *et al.* 1994; Xiong & Steringer, 2000). The pH level in the extracellular space was lower than that in the perfusate (7.35 ± 0.04), probably reflecting a gradient in P_{CO_2} across the thickness of the hippocampal isolate as suggested by Voipio & Kaila (1993). Extracellular K^+ activity measured from the centre of the hippocampal isolate was 4.05 ± 0.04 mM ($n = 10$), very close to the K^+ level in the perfusate (3.5 mM). Unlike the slow oscillations observed from cat neocortex *in vivo* (Amzica & Steriade, 2000), the spontaneous CA1 field rhythms were not associated with detectable fluctuation in extracellular K^+ activity. However, repetitive stimulation of the Schaffer collateral pathway (20 Hz, 1 s) readily raised extracellular K^+ to 7.21 ± 0.33 mM ($n = 6$), in parallel to the appearance of large amplitude bursting field responses (Fig. 2*B*). The stable baseline and the transient rise of extracellular K^+ activity following the afferent stimulation are comparable to the previous study in rat hippocampal slices (Avoli *et al.* 1996). Collectively, the measurements with ion-sensitive electrode were in keeping with the extracellular and single cell recordings mentioned above, further suggesting that the mouse hippocampal isolate retained a state of relatively normal ionic homeostasis.

For morphological examination, the mouse hippocampal isolate was obtained from 28-day-old mice ($n = 4$) and maintained at 31–32 °C for ~4 h and then fixed, re-sectioned and stained with cresyl violet. Viewing under a light microscope, cells in CA1 stratum pyramidale showed no evident abnormalities such as swelling, irregular cell bodies or darkly stained cytoplasmic particles (Fig. 2*C*).

In several preliminary experiments, we have examined the effects of brief hypoxia on the mouse hippocampal isolate as a positive control (Shen *et al.* 2000). A brief hypoxic episode was induced by exposing the hippocampal isolate to the ACSF aerated with 95 % N_2–5 % CO_2 rather than 95 % O_2–5 % CO_2 for ~3 min (Zhang & Krnjevic, 1993, Perez-Velazques & Zhang 1994; Chung *et al.* 1998). In all isolated hippocampal tissues examined ($n = 15$), spontaneous field rhythms and evoked synaptic potentials in the CA1 were reversibly suppressed by the hypoxic episode, in addition a rise of extracellular K^+ to 6–7 mM and tissue acidification to pH ⩽ 7.05 was noted. These data further indicate that the spontaneous rhythmic field potentials we observed were not a consequence of hypoxia.

In this report we present the data collected from the hippocampal isolate prepared from 21–28-day-old mice because at this developmental stage morphological and electrophysiological properties of rodent hippocampal neurons are near mature levels (Zhang *et al.* 1991; Spigelman *et al.* 1992; Ben-Ari *et al.* 1997; Gomez-Di Cesare *et al.* 1997). We have observed similar spontaneous field rhythms in younger (⩾ 11 days) but not in neonatal (< 10 days) mouse hippocampal tissues (Wu *et al.* 1999). Experiments are currently under way in our laboratory to characterize the developmental profile of these rhythms in the mouse hippocampus.

We also observed spontaneous field rhythms and evoked synaptic field potentials in the hippocampal isolate obtained from C57Bl mice of 29–35 days old (Fig. 2*D*). However, there was noticeable inconsistency in obtaining stable electrophysiological responses and intact morphology from the old mouse hippocampal isolate. It is uncertain whether the failure was due to dissection damage, limited perfusion, or both. Nevertheless, we noted a trend that the lack of the spontaneous rhythm was often in parallel to

the poor field responses following afferent stimulation, suggesting that the failure was associated with impaired glutamatergic transmission. Therefore, although the more developed mouse hippocampal isolate is able to sustain the spontaneous field rhythms *in vitro*, further work is needed to control and improve our experimental variables before they can be thoroughly studied.

Generation mechanisms of spontaneous slow rhythm

We conducted simultaneous extracellular and single cell recordings in the CA1 to reveal an intracellular correlate of the spontaneous field rhythms. Individual cells were sampled in the whole-cell configuration using a 'blind' approach method (Zhang *et al.* 1991, 1994, 1998). The distance between the extracellular and single cell recording sites was estimated to be $\leqslant 0.5$ mm. The recorded cells were filled with neurobiotin during whole-cell dialysis and their morphology was examined after fixation and re-sectioning of the hippocampal isolate. Pyramidal neurons and inhibitory INs were recognized by their electrophysiological and morphological properties (see Methods).

Monitored at voltages near the resting potential (approximately −60 mV), CA1 pyramidal neurons exhibited periodic IPSPs (or IPSCs in voltage-clamp recordings) or a mixture of EPSP–IPSP. The IPSPs/IPSCs component became dominant while holding the neurons at more

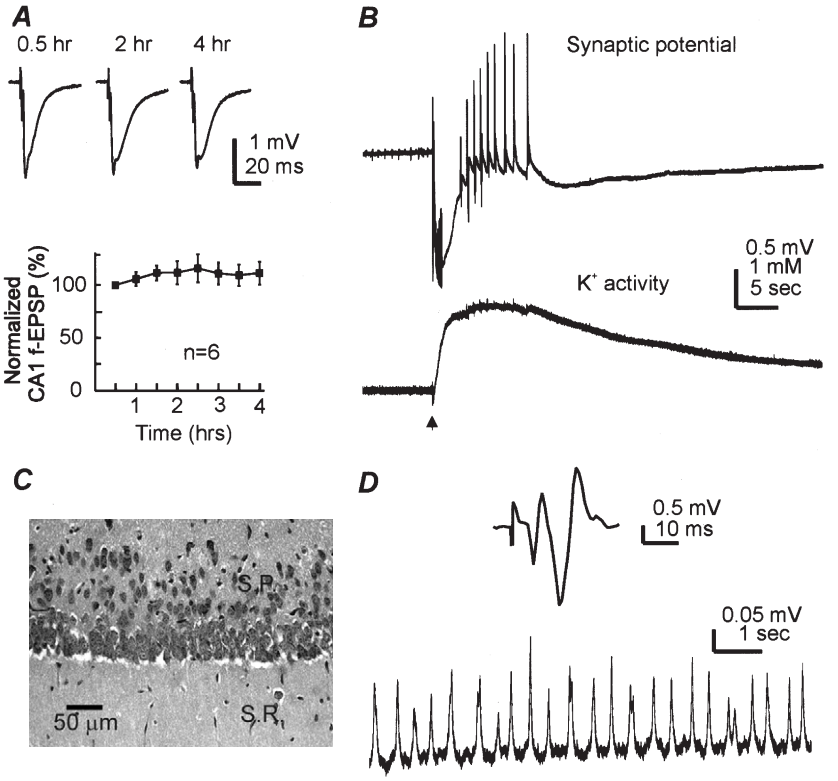

Figure 2. Electrophysiological and morphological integrity

A top, field EPSPs were evoked from the CA1 dendritic areas of a 24-day-old mouse hippocampal isolate by constant Schaffer collateral stimulation every 30 s. Representative traces were collected at three indicated times after placing the tissue in the recording chamber. Each trace was an average from three consecutive measurements. Bottom, amplitudes of CA1 dendritic field EPSPs were measured from six hippocampal tissues (22–27 days old), and the measurements were normalized and plotted *vs.* the recording time. Data points represent means ± S.E.M. from a 5 min period. The responses sampled ~30 min after placing the tissue into the recording chamber were taken as the baseline (2.11 ± 0.18 mV). *B*, simultaneously collected records showing rhythmic field potentials (top) and the measurement of extracellular K^+ activity (bottom) from a 25-day-old mouse hippocampal isolate. The repetitive stimulation of the Schaffer collateral pathway (arrow, 20 Hz, 1 s) induced an initial negative (downward) shift in the extracellular potential and subsequently multiple bursting field responses. The changes in extracellular potentials were in parallel with a rise of extracellular K^+. Baseline level of external K^+ was 3.9 mM. *C*, a photo from a cresyl violet-stained tissue section showing morphology of CA1 cells. Isolated hippocampal tissues ($n = 4$) were obtained from 28-day-old mice. These tissues were maintained i*n vitro* at 32°C for 4 h and then fixed and re-sectioned (6 μm thickness). Abbreviations: S.R., stratum radiatum; S.P., stratum pyramidale. *D*, records were collected from a 35-day-old mouse hippocampal isolate. Top, an averaged trace showing the synaptic field potential evoked from the CA1 somatic area. Bottom, spontaneous field rhythms sampled from the same recording site.

positive potentials (−50 to −40 mV), without altering the temporal relation between the IPSPs/IPSCs and the field rhythms. We analysed the phase relation between the pyramidal IPSPs/IPSCs and field rhythms, taking the peaks of the rhythmic field potentials as reference (zero-phase shift). In a majority of CA1 pyramidal neurons examined (28 of 37), the phase shift of IPSPs/IPSCs *vs.* the nearby rhythmic field potential was ⩽ 5 deg per rhythm cycle (Fig. 3*A*). Dual whole-cell recordings revealed that during the spontaneous field rhythms, rhythmic IPSPs/IPSCs occurred synchronously in spatially separated pyramidal neurons (recording sites of ~0.5 mm apart, 3 pairs; Fig. 5*A* and *B*). We suggest that based on these observations the spontaneous CA1 field rhythms largely represent a summation of IPSPs from a population of pyramidal neurons.

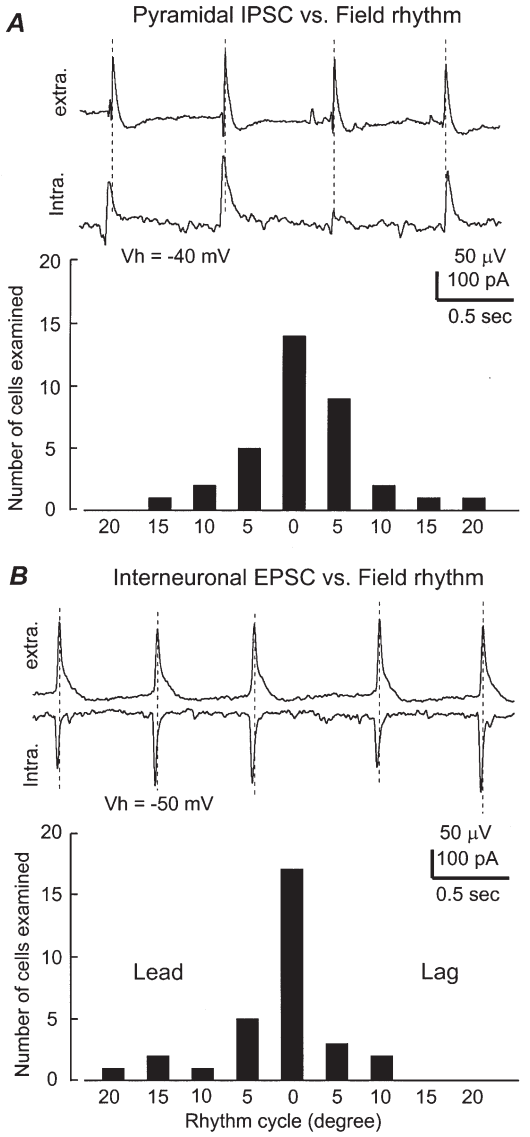

Figure 3. Phase relation of single cell responses *vs.* field rhythms

A top, simultaneously collected field rhythm and pyramidal IPSCs from a 24-day-old mouse hippocampal isolate. The pyramidal neuron was voltage clamped at −40 mV. Dashed lines were drawn to mark the peaks of the rhythmic field potentials. Bottom, summary of the phase relation of pyramidal cell IPSP/IPCS *vs.* the field rhythms. *X*-axis, rhythm cycle binned every 5 deg, taking the peak of rhythmic field potentials as reference (zero-phase shift). *Y*-axis, number of neurons within each bin. *B* top, CA1 field rhythms and interneuronal EPSCs simultaneously recorded from a 22-day-old hippocampal isolate. The interneuron was voltage clamped at −50 mV. Bottom, the phase relation of interneuronal EPSPs/EPSCs *vs.* field rhythms.

We next examined the ionic and pharmacological features of IPSPs recorded from pyramidal neurons. Gramicidin-perforated whole-cell recordings were used to measure the reversal potential of the IPSPs/IPSCs because membrane perforation by gramicidin is thought to be impermeable to Cl^- thus minimizing the measurement errors arising from Cl^- exchanges between cytoplasm and patch pipette solution (Rhee *et al.* 1994). By holding the neurons at different voltages, the estimated reversal potential for the rhythmic IPSPs/IPSCs was −68 ± 1.8 mV ($n = 5$ cells, Fig. 4), which was in the range predicted for the Cl^--dependent IPSPs in CA1 pyramidal neurons (Zhang *et al.*

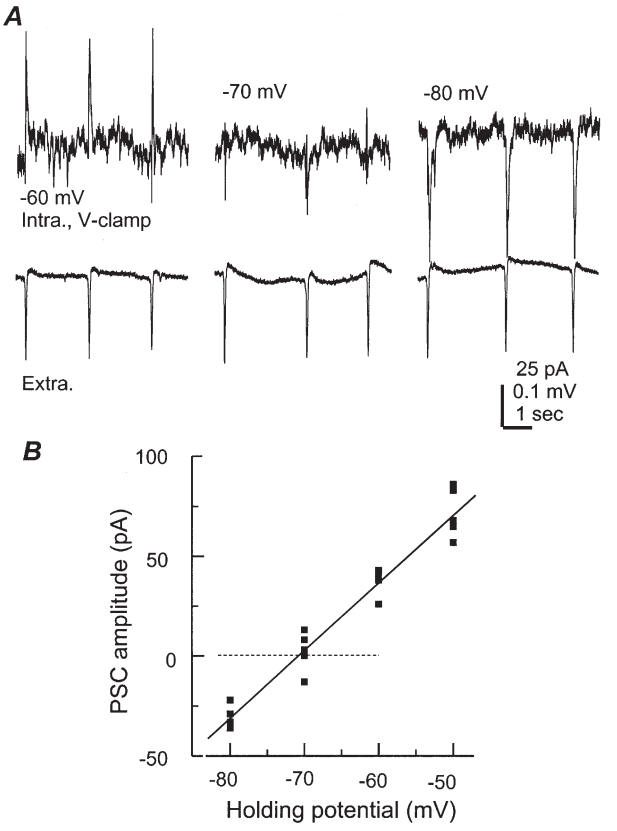

Figure 4. Measurement of IPSC reversal potential

A, periodic IPSCs (top) and nearby rhythmic field potentials (bottom) simultaneously collected from a 21-day-old hippocampal isolate. The pyramidal neuron was recorded using the perforated (gramicidine) method and voltage clamped at different potentials as indicated. *B*, the amplitudes of IPSCs were measured and then plotted *vs.* the corresponding holding potentials. The line through data points was a linear regression fit ($r = 0.97$).

1991). Pharmacologically, the pyramidal IPSPs/IPSCs and the coherent field rhythms were reversibly abolished by perfusion of the hippocampal isolate with the $GABA_A$ receptor antagonist bicuculline methiodide (5–10 μM, $n = 6$, Fig. 5*A*), but not by $GABA_B$ receptor antagonist CGP55845 (10 μM, $n = 4$). Thus, the rhythmic IPSPs/IPSCs that correlate with the spontaneous field rhythms were mediated by synaptic activation of $GABA_A$ receptors. During washing out of bicuculline and prior to the return of slow field rhythms, we often observed large amplitude bursting field responses that occurred spontaneously and lasted for 10–30 s. In parallel to the bursting field potentials, prolonged depolarization superimposed with clusters of discharges was found to occur synchronously in pyramidal neurons (Fig. 5*C*). These bursting responses are similar to the epileptiform activity observed from rat hippocampus *in vivo* (Bragin *et al.* 1997; Galvan *et al.* 2000). Based on these observations we further suggest that the baseline spontaneous field rhythms are supported by balanced interactions between GABAergic inhibitory and glutamatergic excitatory systems.

If spontaneous field rhythms largely reflect the GABAergic IPSPs originating from a population of pyramidal neurons as we propose above, one would expect that GABAergic inhibitory INs would exhibit periodical excitatory responses in correlation with the field rhythms. Indeed, all inhibitory INs ($n = 32$) sampled from the CA1 subfields, such as oriens/alveus, pyramidale or radiatum area, displayed periodic EPSPs (or EPSCs in voltage clamp,) or EPSPs superimposed with spikes while monitored at voltages near the resting membrane potential (approximately −50 mV, Fig. 6*A*). These EPSPs/EPSCs occurred in a close-phase relation with the nearby recorded field rhythms (Fig. 3*B*), but discharging individual INs by intracellular injection of depolarizing current pulses did not induce a field response or alter the on-going rhythmic field potentials recorded nearby. Synchronized EPSPs/ discharges were also found

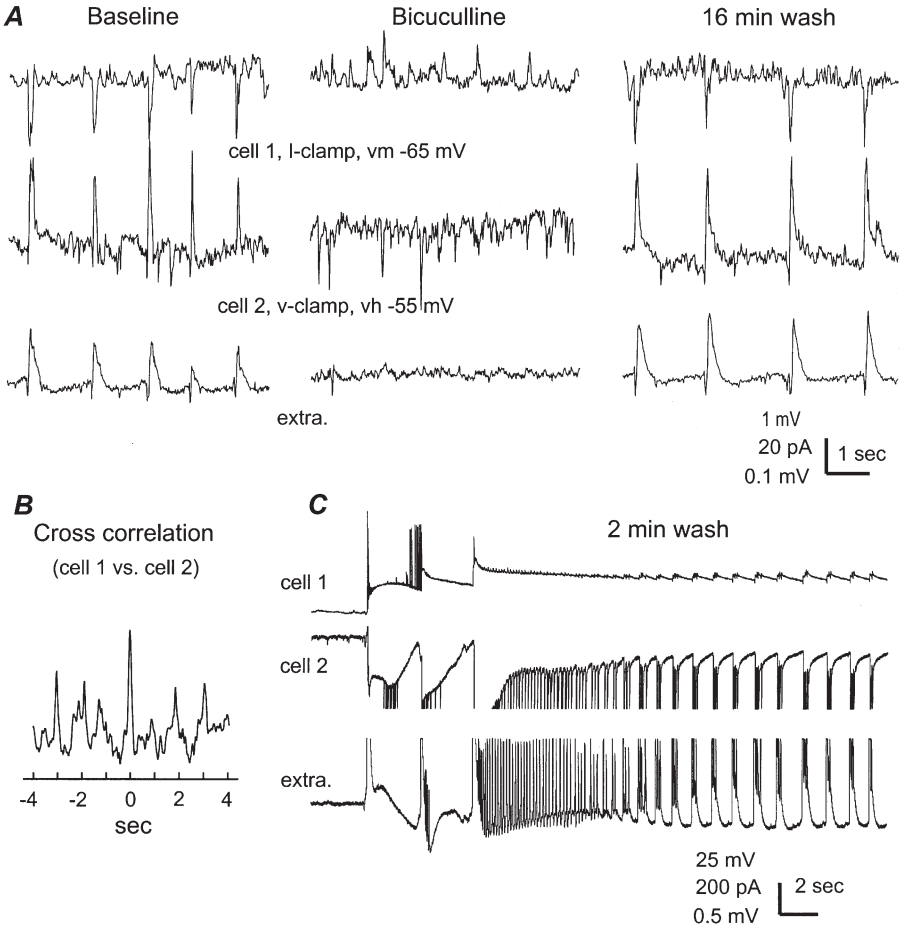

Figure 5. $GABA_A$ receptor-mediated synchronous IPSPs/IPSCs in pyramidal neurons

All records were collected from a 21-day-old hippocampal isolate via dual whole-cell recordings plus extracellular monitoring of CA1 field rhythms. Cell 1 (top) was monitored in current-clamp mode at the resting potential and cell 2 (middle) was voltage clamped at −55 mV. *A*, responses collected before, at the end of perfusion of bicuculline methiodide (BMI, 10 μM, ~5 min) and after 16 min of wash. *B*, the cross correlation plot was generated from the baseline intracellular responses. *C*, spontaneous bursting responses collected after ~2 min of wash. Parts of extracellular and the cell 2 responses (~4 s after the start of the bursting activity) were truncated due to saturation of the digitizer.

in simultaneously recorded INs (2 pairs, Fig. 6*B*) during the course of spontaneous field rhythms. Based on our observations and divergent GABAergic innervation of hippocampal pyramidal neurons previously demonstrated (Buhl *et al.* 1994; Cobb *et al.* 1995), we suggest that the synchronous discharges of GABAergic INs impose the rhythmic IPSPs onto a population of pyramidal neurons thereby mediating the rhythmic field potentials. Presumed glia cells ($n = 11$), characterized by a resting potential more negative than −70 mV, low input resistance ($\leqslant 15$ MΩ) and lack of synaptic response and action potential, exhibited no rhythmic fluctuation in membrane potential. The lack of detectable glia rhythmicity during the spontaneous field rhythms is consistent with our view that the spontaneous field rhythms are primarily of synaptic origin.

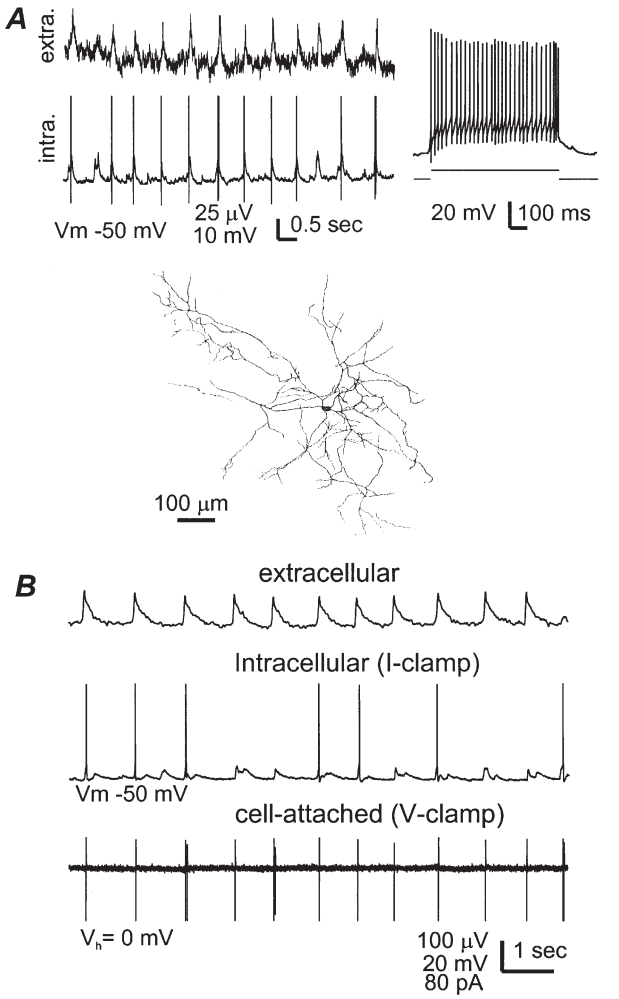

Figure 6. Rhythmic excitation of inhibitory interneurons

A top-left, field rhythms and interneuronal EPSP/discharges simultaneously recorded from a 24-day-old hippocampal isolate. The interneuronal spikes were truncated for illustration purpose. Top-right, discharges of the interneuron induced by intracellular injection of a depolarizing current pulse. Bottom, camera lucida tracing of the recorded interneuron. Neurobiotin-stained signals were visualized from four horizontal sections (100 μm in thickness) in stratum radiatum and superimposed. *B*, data collected from a 17-day-old hippocampal isolate via extracellular monitoring together with dual cell recordings from interneurons in CA1 oriens/alveus region. One interneuron was recorded in the current-clamp configuration at the resting potential (middle) and another was monitored at rest ($V_h = 0$) via the cell-attached voltage-clamp configuration (bottom). Note the synchronized excitatory responses in the two interneurons, i.e., EPSP/discharges in the middle panel and spiking currents in the bottom panel.

To explore whether GABAergic field rhythms can be induced by maintained excitation of hippocampal neurons, we perfused the mouse hippocampal isolate with *trans*-(1*S*,3*R*)-ACPD (*trans*-ACPD, 50 μM), a powerful agonist for the metabotropic glutamate receptors. Application of *trans*-ACPD caused a brief appearance of fast oscillatory activities (10–30 Hz, lasting 10–20 s), in keeping with the previous study in rat hippocampal slices (Whittington *et al.* 1995). As the perfusion of *trans*-ACPD continued, we observed bursting field potentials in the CA3 and CA1 regions, with amplitudes of 1–2 mV and occurrence frequencies of 0.1–0.5 Hz (Fig. 7*B*). Adding CNQX (10 μM) to the ACPD-containing ACSF abolished the bursting responses, revealing some irregular and small ($\leqslant 30$ μV) field potentials in two of the four tissues examined (Fig. 7*C*). These irregular responses were further suppressed by adding bicuculline methiodide (10 μM) into the perfusate (Fig. 7*D*), suggesting that their mediation might involve the activity of $GABA_A$ receptors. We also examined the effects of high external K^+ on the mouse hippocampal isolate by raising KCl from 3.5 to 8 mM while keeping the rest of the ACSF components unchanged. Bursting field potentials, similar to those induced *trans*-ACPD, were also observed in the mouse hippocampal isolate ($n = 3$) following exposure to the high K^+ ACSF. However, in the presence of high K^+ and 10 μM CNQX, there was no detectable rhythmic field potential in the CA3 and other hippocampal regions. Thus, maintained excitation via pharmacological stimulation of metabotropic glutamate receptors is capable of initiating GABAergic field responses in the mouse hippocampal isolate, but the induced responses are much less consistent and smaller than the spontaneously occurring field rhythms. Collectively, these observations further suggest that the glutamatergic drive mediated by AMPA receptors is crucial in sustaining and synchronizing the GABAergic population rhythms in the mouse hippocampal isolate.

Muscarinic induction of θ-like rhythms

The hippocampus expresses high levels of muscarinic receptors (Levey *et al.* 1995) and receives cholinergic projections from the medial septum and the diagonal band of Broca (Lewis & Shute, 1967; Saper, 1984; Frotscher & Leranth, 1985). The septo-hippocampal cholinergic system is known to play a crucial role in controlling hippocampal EEG rhythms (Buzsáki *et al.* 1983; Bland & Colom, 1993; Vinogradova, 1995), particularly the transition from LIA

to RSA (θ rhythms, Bland *et al.* 1999). Pharmacological stimulation of muscarinic receptors has been shown to induce θ oscillations in rodent hippocampal slices via network activity involving GABAergic INs (Konopacki *et al.* 1987; MacVicar & Tse, 1989; Huerta & Lisman, 1993, 1996; Williams & Kauer, 1997; Chapman & Lacaille, 1999; Fisahn *et al.* 1999).

If the spontaneous field rhythms we observed represent intrinsic network activity of the hippocampus, one would expect modifications following pharmacological stimulation of muscarinic receptors. To test this, we perfused the hippocampal isolate with a cholinergic agonist carbachol (10 μM, 6–8 min). The application of carbachol caused an initial inhibition of the spontaneous slow-field rhythms and a subsequent emergence of fast oscillations in the θ band (6–12 Hz). The fast θ oscillations gradually increased their amplitudes, and then intermixed with the large amplitude ($\geqslant$ 0.5 mV) bursting field potentials that occurred every 8–15 s (n = 5, Fig. 8*A*). The θ oscillations–bursting responses were reversible after washing out carbachol for 15–20 min and reproducible after re-application of carbachol. Simultaneous extracellular and single cell recordings revealed that CA1 pyramidal neurons displayed small amplitude, mixed EPSPs–IPSPs during the carbachol-induced θ oscillations, which were in a sharp contrast to the regular large amplitude IPSPs that correlated with the baseline slow-field rhythms (Fig. 8*B*). Pre-perfusion of the hippocampal isolate with atropine (3 μM, n = 3), a general but potent muscarinic receptor antagonist, did not interrupt

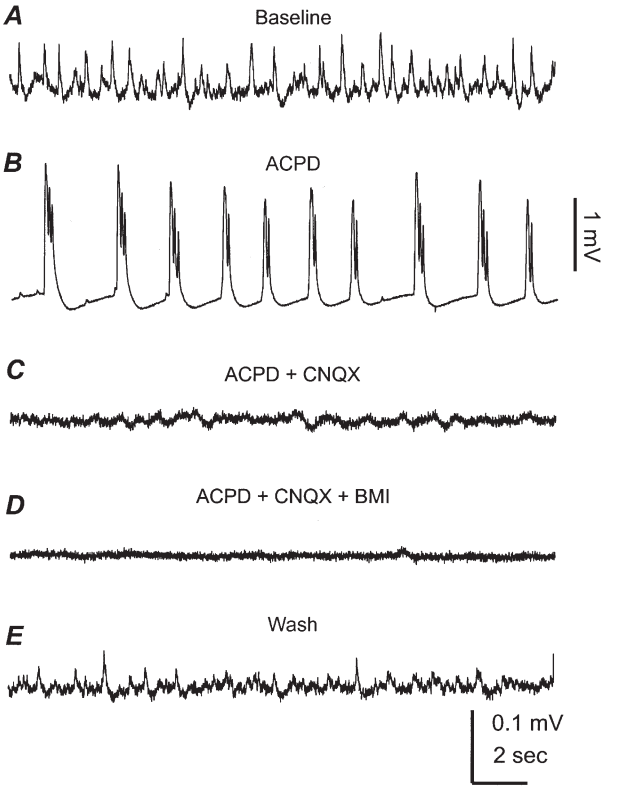

Figure 7. Field responses induced by *trans*-(1*S*,3*R*)-ACPD (ACPD)

All extracellular records were collected from the CA3 region of a 25-day-old mouse hippocampal isolate. *A*, baseline control. *B*, bursting field potentials collected at the end of ACPD perfusion (50 μM, 8 min). *C*, CNQX, 10 μM was added into the ACPD-containing perfusate and the record was collected after co-application of ACPD and CNQX for ~8 min. *D*, Bicuculline, 10 μM methiodide (BMI) was added into the ACPD + CNQX-containing perfusate, and the record was collected after co-application of the three agents for 8 min. *E*, after washing out the above agents for ~50 min.

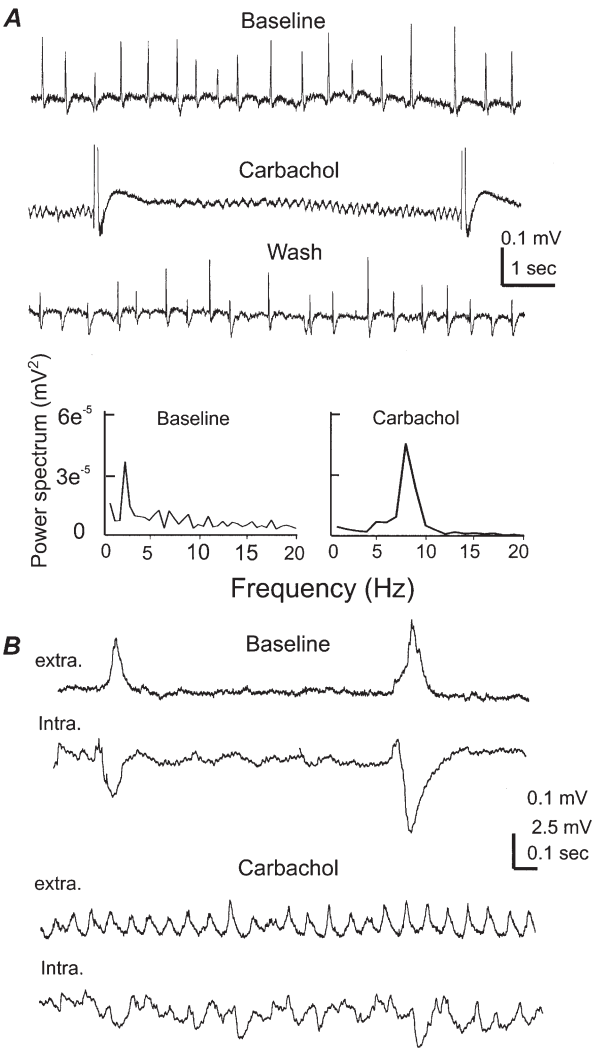

Figure 8. Muscarinic stimulation of θ oscillations

A, extracellular responses were collected from the CA1 region of a 24-day-old hippocampal isolate. Representative records were sampled before, at the end of carbachol application (10 μM, 8 min) and after washing out carbachol. Large amplitude bursting responses induced by carbachol were truncated for illustration purpose. The fast rhythmic events sampled between the adjacent bursting responses (middle) were used to generate the carbachol power spectrum plot. *B*, records were collected from a 21 days old hippocampal isolate. CA1 field rhythms and intracellular responses of a nearby pyramidal neuron were sampled simultaneously. Membrane potentials of the pyramidal cell were about −57 mV before, and −52 mV after perfusion of 10 μM carbachol.

the spontaneous slow-field rhythms but prevented the effects of subsequently applied carbachol ($n = 3$).

The induction of muscarinic θ oscillations is similar to previous studies in slices, demonstrating that the network of the mouse hippocampal isolate is highly sensitive to modulation by muscarinic and perhaps other neurotransmitter receptors. A thorough examination of muscarinic effects on hippocampal rhythms is beyond the focus of the present study. Nevertheless, we speculate that suppression of synaptic transmission (Pitler & Alger, 1992; Behrends & ten Bruggencate, 1993) and blockade of several K^+ currents (Madison *et al.* 1987; Dutar *et al.* 1995) might, in part, be responsible for the muscarinic inhibition of the slow-field rhythms and induction of θ oscillations. It remains to be determined whether distinct populations of GABAergic INs react differently following muscarinic stimulation (McMahon *et al.* 1998; Parra *et al.* 1998) thus accounting for the complex of rhythmic field responses we observed after the application of carbachol.

Propagation and regional generation of slow-field rhythms

To explore the spatial distribution of the CA1 slow-field rhythms, extracellular recordings were made simultaneously from the ventral, middle and dorsal regions of the hippocampal isolate. The adjacent recording sites were ~1.5 mm apart. Rhythmic field potentials of 1.9 ± 0.2 Hz were observed from the three recording sites with a temporal sequence in which the ventral responses preceded those in the dorsal region by 21.7 ± 1.5 ms ($n = 5$, Fig. 9*A*). After obtaining stable baseline recordings, we made two transverse cuts to separate the three recording sites and then monitored corresponding regional responses. Rhythmic field potentials were found to occur spontaneously from each of the disconnected areas, though they were not as stable and regular as the baseline controls. In addition, there was no temporal correlation among these regional field rhythms (Fig. 9*B*). The frequencies of these regional rhythms varied widely presumably influenced by the extent of mechanical/chemical disturbances associated with the cut and the recovery processes of disconnected areas. Although not statistically significant, after the cut the ventral and middle rhythmic field potentials appeared to be faster (0.6–1.9 Hz) than the dorsal responses (0.3–1.4 Hz). Collectively, these observations suggest that in the hippocampal isolate *in vitro* the spontaneous CA1 field rhythms are driven by the ventral region and propagate towards the dorsal pole.

To explore the regional rhythmicity of the CA1 or CA3, we made a longitudinal cut that surgically separated these two

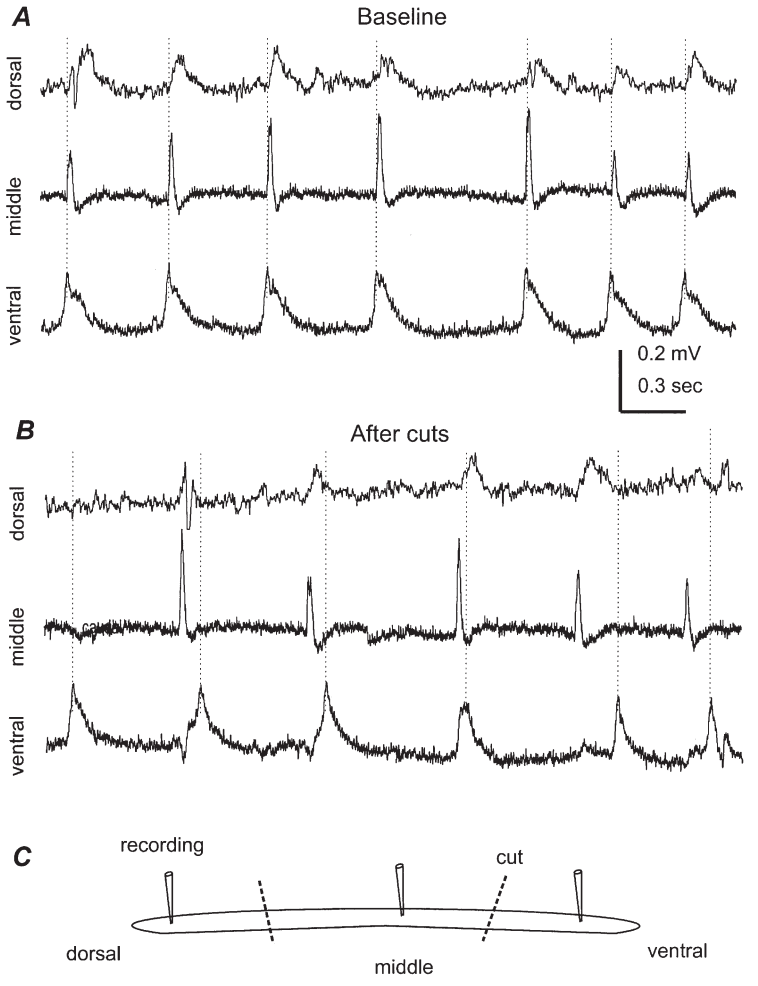

Figure 9. Ventral-to-dorsal spread of spontaneous field rhythms

All records were collected from the CA1 region of a 21-day-old hippocampal isolate. *A*, field rhythms recorded simultaneously from the ventral, middle and dorsal areas of the hippocampal isolate. The distance between adjacent recording sites was ~1.5 mm. Dotted lines were drawn to mark the peaks of ventral responses. *B*, responses sampled ~45 min after two cuts that separated the three recording sites. *C*, a schematic illustration of the recording and cutting arrangement.

regions (see the schematic illustration in Fig. 10). In a set of six tissue strips that contained the CA1 only, extracellular recordings revealed no spontaneous rhythmic potentials, however, repetitive stimulation of CA1 local circuitry (20 Hz, 1 s) could induce periodic field potentials of 2–4 Hz that lasted for 10–20 s (Fig. 10*A*). In contrast, spontaneous rhythmic field potentials of 2.61 ± 0.52 Hz and 20–50 μV were observed in five of six tissue strips that contained the CA3 only. The regional CA3 rhythms were reversibly blocked by 10 μM bicuculline methiodide or 5 μM CNQX ($n = 2$ each, Fig. 10*B*), in keeping with pharmacological properties of the spontaneous field rhythms observed from the entire hippocampal isolate. Thus, functional CA3-to-CA1 projections appear to be essential for the appearance of CA1 spontaneous field rhythms in the intact hippocampal isolate. However, caution should be taken when interpreting the present observations because the extent of mechanical/chemical disturbance associated with the surgical cut and the subsequent recovery process might be different between the CA1 and CA3 thereby influencing the genesis of regional field rhythm. For instance, the pyramidal neurons of the CA3 express a relatively low level of NMDA receptors (Cotman *et al.* 1987) but a high level of K-ATP channels (Mourre *et al.* 1989) as compared with those in the CA1. It remains to be determined whether these factors and others that help reduce Ca^{2+} entry and make the CA3 pyramidal neurons more resistant to the cut insult, and thus help the preservation of CA3 local rhythmicity, as opposed to what was seen in the CA1 region.

DISCUSSION

We demonstrate that it is possible to isolate relatively intact hippocampal tissues from 21–28-day-old mice while preserving their electrophysiological and morphological integrity *in vitro*. Our major findings are the following. (1) Rhythmic field potentials of 0.5 to ⩽ 4 Hz occur spontaneously and propagate throughout the hippocampal isolate. (2) These rhythms are inhibitory in nature, requiring the network activity of GABAergic INs. (3) Activation of muscarinic receptors induces fast oscillations in the θ band.

Large-scale network connectivity is required for sustaining spontaneous population oscillation *in vitro*

Buzsáki *et al.* (1989) have examined the hippocampal synaptic activity in rats 3–5 months after aspiration of subcortical afferents including the fimbria–fornix, ventral hippocampal commissure and suprocallosal inputs. They found that pyramidal neurons of the denervated hippocampus initiated spontaneous, synchronous interictal potentials that could oscillate at 1–2 Hz. The authors suggested that in the intact brain, hippocampal activity is under inhibitory control of subcortical afferent inputs and removal of such tonic inhibition allows extreme synchronization and reverberation of synaptic activity which leads to synchronous interictal activity. More recently, Timofeev *et al.* (2000) have reported that slow cortical oscillations of ⩽ 1 Hz, similar to those seen in intact cortex during slow-wave sleep, could occur spontaneously in deafferented cortical slabs that contained an isolated gyrus, but such slow oscillations were absent in the smaller

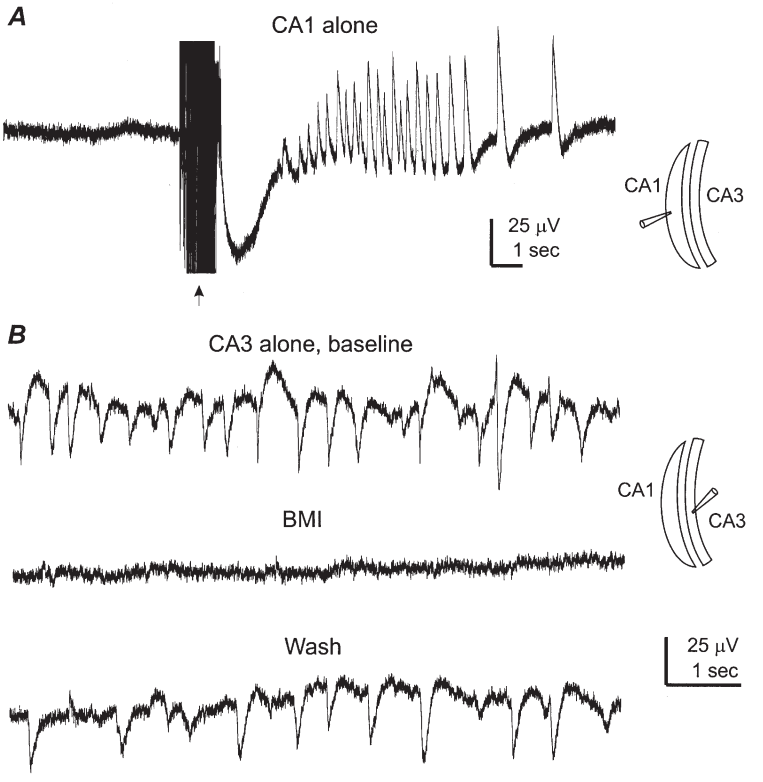

Figure 10. Regionally originated rhythmic field potentials

Hippocampal tissues were prepared from two mice aged 21 days old. *A*, extracellular record was collected from a CA1 tissue strip, showing no spontaneous- but evoked-field responses following repetitive stimulation of local circuitry (arrow, 20 Hz, 1 s). The recording setting and the longitudinal cut were schematically illustrated (right). *B*, extracellular records collected from a CA3 tissue strip before, following perfusion of bicuculline methiodide (BMI, 10 μM, 5 min) and after washing out bicuculline.

cortical slabs. Although the generation of oscillatory activities in hippocampus and neocortex may involve different mechanisms, it appears to be a common phenomenon that a relatively large scale network connectivity is essential for spontaneous population oscillation to occur in the mammalian CNS. (But see Sanchez-Vives & McCormick (2000) for observations of slow oscillations in ferret neocortical slices).

In the mid eighties Schwartzkroin and co-authors observed spontaneous rhythmic synaptic events of 2–4 Hz in slices from the mesial temporal lobe of epileptic patients or hippocampi of normal monkeys (Schwartzkroin & Knowles, 1984; Schwartzkroin & Haglund, 1986). Their data demonstrated that the major component of these rhythmic events was $GABA_A$ receptor-mediated IPSPs that occurred synchronously between pyramidal neurons. They concluded that the spontaneous rhythmic events were not epileptic in nature but rather dependent upon inhibitory IN circuitry. In addition, the spontaneous rhythmic events were observed only in thicker (600–700 μm) but not in thinner conventional (300–500 μm) slices. It was suggested that the circuitry required for the spontaneous rhythmic events might be interrupted when the thin slice was made (Schwartzkroin & Haglund, 1986). Since that time, although rhythmic activities of 0.5 to $\leqslant$ 4 Hz have been induced pharmacologically (Schneiderman, 1986; Miles & Wong, 1987; Avoli *et al.* 1996; Zhang *et al.* 1998; Fellous & Sejnowski, 2000), there has been no reported observation of consistent spontaneous population rhythms in the conventional rodent hippocampal slice. We report here that by preserving the divergently distributed CA3-to-CA1 circuitry, the mouse hippocampal isolate displayed spontaneous rhythmic field potentials of 0.5 to $\leqslant$ 4 Hz without any ionic or pharmacological manipulation. Our observations, together with the early studies in rat hippocampus *in vivo* (Buzsáki *et al.* 1989) and in slices (Schwartzkroin & Knowles, 1984; Schwartzkroin & Haglund, 1986), provide compelling evidence that the hippocampal circuitry can generate spontaneous population oscillations if sufficient neuronal connectivity is retained.

Generation of spontaneous field rhythms by GABAergic IN networks

We propose that the spontaneous field rhythms largely represent a summation of IPSPs originating from a population of pyramidal neurons, which results from the synchronous discharges of GABAergic INs. Our view is based on the following observations. (1) The spontaneous field rhythms (30–300 μV) were several times smaller in amplitude than evoked glutamate synaptic field potentials, making it more consistent with population GABAergic activity. (2) The field rhythms correlated closely with IPSPs recorded from individually recorded pyramidal neurons and both of the events were blocked by $GABA_A$ receptor antagonist, bicuculline methiodide. (3) Inhibitory INs displayed synchronous excitatory responses coherent with the field rhythms, but intracellular stimulation of individual IN did not produce a field response or interrupt the on-going field rhythms, suggesting the dominant role of networked INs in initiating the spontaneous field rhythms.

The issue of how the spontaneous inhibitory rhythms are generated remains to be further investigated. Our data suggest that the rhythms could not be mimicked by maintained excitation via raising external K^+ or stimulating metabotropic glutamate receptors in the presence of CNQX. In the light of the well-described synaptic circuitry in the hippocampal proper (Amaral & Witter, 1989; Freund & Buzsáki, 1996), we suggest the following network scheme for genesis of the spontaneous inhibitory rhythms. In the hippocampal isolate, GABAergic INs may receive both feed-forward and recurrent glutamatergic inputs, such as via the Schaffer collateral pathway and recurrent axons of pyramidal neurons. Axon terminals from a group of pyramidal neurons may converge on individual IN (Buhl *et al.* 1994; Cobb *et al.* 1995). Thus, although individually recorded pyramidal neurons fire sparsely in our experiments, pyramidal neurons as a population can participate actively in IN spike generation, particularly via the interaction of glutamatergic EPSPs and voltage-gated ion channels on IN dendrites (Traub, 1995; Martina *et al.* 2000). In addition, GABAergic INs themselves interconnect synaptically (Gulyás *et al.* 1996; Hájos & Mody, 1997) or electrically via gap junction communication (Michelson & Wong, 1994; Zhang *et al.* 1998; Galarreta & Hestrin, 1999; Gibson *et al.* 1999; Fukuda & Kosaka, 2000; Hormuzdi *et al.* 2001; Deans *et al.* 2001). These reciprocal connections may help to recruit and stabilize IN synchrony (Wang & Rinzel, 1992; Traub, 1995; Jefferys *et al.* 1996; Skinner *et al.* 1999) therefore playing important roles in controlling network rhythms. In this regard, INs via network activity may function to impose coherent IPSPs onto a population of pyramidal neurons, hence mediating the spontaneous field rhythms. To verify this hypothetical scheme, it is of great interest to explore how GABAergic inhibitory INs interact during the spontaneous rhythms and what are the participating neurochemical mechanisms which maintain it in the δ frequency band (0.5 to $\leqslant$ 4 Hz).

Propagation and regional origination of the spontaneous field rhythms

Our data show that although the spontaneous field rhythm could arise regionally, the rhythm propagates along the longitudinal axis of the hippocampal isolate from the ventral towards the dorsal pole. During each rhythm cycle the ventral responses preceded the dorsal response by a mean time interval of ~22 ms over a distance of ~3 mm. The calculated propagation speed (0.13 m s^{-1}, assuming linearity) was slower than the axon conduction velocity of CA3 pyramidal neurons (~0.5 m s^{-1}, Miles *et al.*

1988), suggesting a spread via multiple synapses. The physiological significance and mechanisms that underlie the ventro–dorsal spread of the *in vitro* rhythms remain to be elucidated. We have explored the possible roles of inhibitory synaptic connections in the propagation of the *in vitro* hippocampal rhythms using a phase-coupled oscillator model (Skinner *et al.* 2001). Our simulation data suggest that the relative coupling strength of adjacent groups of inhibitory INs influence the direction of rhythm propagation. Detailed assessments of the propagation profile and the properties of regionally distributed GABAergic IN are needed to verify these theoretical predictions.

We found no detectable field rhythm in the CA1 region alone after a longitudinal surgical cut that separated the CA1 and CA3. In contrast, the CA3 region alone was able to sustain spontaneous, bicuculline-sensitive rhythmic field potentials. Thus, in the intact hippocampal isolate the spontaneous field rhythms appear to originate from the CA3, whereas functional CA3-to-CA1 projections are needed to support the CA1 rhythms. This view is consistent with our knowledge about the extensive recurrent axon arbors of CA3 pyramidal neurons (Amaral & Witter, 1989) and the ability of recurrent CA3 excitation to sustain population oscillations in the hippocampal circuitry (Schneiderman, 1986; Miles & Wong, 1987; Buzsáki *et al.* 1989; Traub *et al.* 1989). However, further work is needed to characterize the cellular bases of the spontaneous rhythm in the CA3 and the synaptic physiology of the divergent CA3-to-CA1 projections (Andersen *et al.* 2000).

Significance and experimental implications

Hippocampal EEG recordings from rats (Stumpf, 1965; Vanderwolf, 1969; Buzsáki *et al.* 1983; Leung, 1985; Bland & Colom, 1993) and mice (Caudarella *et al.* 1987; Tsuboi *et al.* 1994) reveal large amplitude irregular activity (LIA) during slow-wave sleep and wake immobility. Spectral analysis indicates that the dominant frequency component of the LIA is in the range of 0.5 to $\leqslant$ 3 Hz (Leung, 1985). The mechanisms that underlie the LIA are not fully understood. The spontaneous field rhythms we observed from the mouse hippocampal isolate share some common features with the hippocampal LIA seen in behaving animals with respect to the low frequency and modulation by muscarinic stimulation. Although by no means does this prove that the *in vitro* rhythms we observed match LIA activity seen in intact animals, our model system may help to explore the cellular and network mechanisms that are potentially involved in generating hippocampal slow rhythms, including those associated with epileptiform activity (Buzsáki *et al.* 1989; Gambardella *et al.* 1995; Normand *et al.* 1995; Galvan *et al.* 2000).

Previous studies have shown that neonatal (< 10 days) rat hippocampal neurons exhibit giant depolarizing potentials (GDP) that occur with a frequency of $\leqslant$ 0.1 Hz (Ben-Ari *et al.* 1989; Cherubini *et al.* 1991). Different from the IPSP-correlated field rhythms we report here, the GDP manifests as synchronized population discharges resulting from synergistic actions of excitatory $GABA_A$ and glutamate AMPA/NMDA receptors (Ben-Ari *et al.* 1997; Leinekugel *et al.* 1997). In the isolated whole neonatal hippocampus, the GDP propagates from the dorsal towards the ventral pole at a speed of 0.008 m s^{-1} (Leinekugel *et al.* 1998), which is much slower than the spread of the spontaneous field rhythms we observed. A common feature shared by the GDP and our observed rhythms is that $GABA_A$ receptors play a central role in mediating both types of activities. We found in our preliminary experiments that the spontaneous field rhythms were detectable in the hippocampal tissues obtained from $\geqslant$11-day-old mice but not in younger animals (Wu *et al.* 1999). Although further characterization is needed, the postnatal appearance of the spontaneous field rhythms is in accordance with the time frame by which the hyperpolarizing, $GABA_A$ receptor-mediated IPSPs establish in immature rodent hippocampal neurons (Zhang *et al.* 1991; Ben-Ari *et al.* 1997). We speculate that the maturation of hyperpolarizing $GABA_A$ IPSPs, together with other factors (Spigelman *et al.* 1992; Gomez-Di Cesare *et al.* 1997) may cause a transition from the GDP to the spontaneously occurring inhibitory field rhythms in the developing hippocampus. Ben-Ari (2001) has postulated that the GDP represent a primitive pattern activity in the neonatal hippocampus functioning to provide a more selective control of synaptic formation. In this context, it is assumed that the transition from the GDP to the dominant inhibitory rhythm may further refine and consolidate the hippocampal network at more developed stages.

In summary, we report here a novel *in vitro* hippocampal preparation. The model system we developed may be suitable for studying various fundamental properties of the hippocampus, including developmental profiles, synaptic plasticity, epileptiform activity and changes induced by metabolic stress. Furthermore, the mouse hippocampal isolate may prove to be a convenient and sensitive model to examine the genetic components involved in hippocampal rhythm generation via the use of transgenic animals. We anticipate that with further use and improvement of this model system, the *in vitro* neurophysiological study of the hippocampus may shift from a focus on local circuitry of the slice to a relatively large-scale network where memory-related information processing is hypothesized to take place (Moser & Moser, 1998).

REFERENCES

Amaral, D. G. & Witter, M. P. (1989). The three-dimensional organization of the hippocampal formation: a review of anatomical data. *Neuroscience* **31**, 571–591.

Ammann, D. (1986). *Ion-Selective Microelectrodes: Principles, Design, and Application.* Springer-Verlag, Berlin.

Amzica, F. & Steriade, M. (2000). Neuronal and glial membrane potentials during sleep and paroxysmal oscillations in the neocortex. *Journal of Neuroscience* **20**, 6648–6665.

Andersen, P., Bliss, T. V. P. & Skrede, K. K. (1971). Lamellar organization of hippocampal excitatory pathways. *Experimental Brain Research* **13**, 222–238.

Andersen, P., Soleng, A. F. & Raastad, M. (2000). The hippocampal lamella hypothesis revisited. *Brain Research* **886**, 165–171.

Andrade, R., Malenka, R. C. & Nicoll, R. A. (1986). A G protein couples serotonin and GABAB receptors to the same channels in hippocampus. *Science* **234**, 1261–1265.

Avoli, M., Louvel, J., Kurcewicz, I., Pumain, R. & Barbarosie, M. (1996). Extracellular free potassium and calcium during synchronous activity induced by 4-aminopyridine in the juvenile rat hippocampus. *Journal of Physiology* **493**, 707–717.

Behrends, J. C. & ten Bruggencate, G. (1993). Cholinergic modulation of synaptic inhibition in the guinea pig hippocampus *in vitro*: excitation of GABAergic interneurons and inhibition of GABA-release. *Journal of Neurophysiology* **69**, 626–629.

Ben-Ari, Y., Cherubini, E., Corradetti, R. & Gaiarsa, J. L. (1989). Giant synaptic potentials in immature rat CA3 hippocampal neurones. *Journal of Physiology* **416**, 303–325.

Ben-Ari, Y., Khazipov, R., Leinekugel, X., Caillard, O. & Gaiarsa, J. L. (1997). GABAA, NMDA and AMPA receptors: a developmentally regulated 'menage a trois'. *Trends in Neurosciences* **20**, 523–529.

Ben-Ari, Y. (2001). Developing networks play a similar melody. *Trends in Neurosciences* **24**, 353–360.

Bland, B. H., Anderson, P. & Ganes, T. (1975). Two generators of hippocampal theta activity in rabbits. *Brain Research* **94**, 199–218.

Bland, B. H. & Colom, L. V. (1993). Extrinsic and intrinsic properties underlying oscillation and synchrony in limbic cortex. *Progress in Neurobiology* **41**, 157–208.

Bland, B. H., Oddie, S. D. & Colom, L. V. (1999). Mechanisms of neural synchrony in the septohippocampal pathways underlying hippocampal theta generation. *Journal of Neuroscience* **19**, 3223–3237.

Bracci, E., Vreugdenhil, M., Hack, S. P. & Jefferys, J. G. (1999). On the synchronizing mechanisms of tetanically induced hippocampal oscillations. *Journal of Neuroscience* **19**, 8104–8113.

Bragin, A., Penttonen, M. & Buzsaki, G. (1997). Termination of epileptic afterdischarge in the hippocampus. *Journal of Neuroscience* **17**, 2567–2579.

Buhl, E. H., Halasy, K. & Somogyi, P. (1994). Diverse sources of hippocampal unitary inhibitory postsynaptic potentials and the number of synaptic release sites. *Nature* **368**, 823–828.

Buzsáki, G. (1989). Two-stage model of memory trace formation: a role for 'noisy' brain states. *Neuroscience* **31**, 551–570.

Buzsáki, G., Leung, L. W. & Vanderwolf, C. H. (1983). Cellular bases of hippocampal EEG in the behaving rat. *Brain Research* **287**, 139–171.

Buzsáki, G., Ponomareff, G. L., Bayardo, F., Ruiz, R. & Gage, F. H. (1989). Neuronal activity in the subcortically denervated hippocampus: a chronic model for epilepsy. *Neuroscience* **28**, 527–538.

Caudarella, M., Durkin, T., Galey, D., Jeantet, Y. & Jaffard, R. (1987). The effect of diazepam on hippocampal EEG in relation to behavior. *Brain Research* **435**, 202–12.

Chapman, C. A. & Lacaille, J. C. (1999). Cholinergic induction of theta-frequency oscillations in hippocampal inhibitory interneurons and pacing of pyramidal cell firing. *Journal of Neuroscience* **19**, 8637–8645.

Cherubini, E., Gaiarsa, J. L. & Ben-Ari, Y. (1991). GABA: an excitatory transmitter in early postnatal life. *Trends in Neurosciences* **14**, 515–519.

Chesler, M., Chen, J. C. & Kraig, R. P. (1994). Determination of extracellular bicarbonate and carbon dioxide concentrations in brain slices using carbonate and pH-selective microelectrodes. *Journal of Neuroscience Methods* **53**, 129–136.

Chung, I., Zhang, Y., Eubanks, J. H. & Zhang, L. (1998). Attenuation of hypoxic current by intracellular applications of ATP regenerating agents in hippocampal CA1 neurons of rat brain slices. *Neuroscience* **86**, 1101–1107.

Cobb, S. R., Buhl, E. H., Halasy, K., Paulsen, O. & Somogyi, P. (1995). Synchronization of neuronal activity in hippocampus by individual GABAergic interneurons. *Nature* **378**, 75–78.

Cotman, C. W., Monaghan, D. T., Ottersen, O. P. & Stormmathisen, J. (1987). Anatomical organization of excitatory amino-acid receptors and their pathways. *Trends in Neurosciences* **10**, 273–280.

Deans, M. R., Gibson, J. R., Sellitto, C., Connors, B. W. & Paul, D. L. (2001). Synchronous activity of inhibitory networks in neocortex requires electrical synapses containing connexin36. *Neuron* **31**, 477–485.

Dolorfo, C. L. & Amaral, D. G. (1998). Entorhinal cortex of the rat: topographic organization of the cells of origin of the perforant path projection to the dentate gyrus. *Journal of Comparative Neurology* **398**, 25–48.

Dutar, P., Bassant, M. H., Senut, M. C. & Lamour, Y. (1995). The septohippocampal pathway: structure and function of a central cholinergic system. *Physiological Reviews* **75**, 393–427.

Fellous, J. M. & Sejnowski, T. J. (2000). Cholinergic induction of oscillations in the hippocampal slice in the slow (0.5–2 Hz), theta (5–12 Hz), and gamma (35–70 Hz) bands. *Hippocampus* **10**, 187–197.

Fisahn, A., Pike, F. G., Buhl, E. H. & Paulsen, O. (1998). Cholinergic induction of network oscillations at 40 Hz in the hippocampus *in vitro*. *Nature* **394**, 186–189.

Freund, T. F. & Buzsáki, G. (1996). Interneurons of the hippocampus. *Hippocampus* **6**, 347–470.

Frotscher, M. & Leranth, C. (1985). Cholinergic innervation of the rat hippocampus as revealed by choline acetyltransferase immunocytochemistry: a combined light and electron microscopic study. *Journal of Comparative Neurology* **239**, 237–246.

Fukuda, T. & Kosaka, T. (2000). Gap junctions linking the dendritic network of GABAergic interneurons in the hippocampus. *Journal of Neuroscience* **20**, 1519–1528.

Galarreta, M. & Hestrin, S. (1999). A network of fast-spiking cells in the neocortex connected by electrical synapses. *Nature* **402**, 72–75.

Galvan, C. D., Hrachovy, R. A., Smith, K. L. & Swann, J. W. (2000). Blockade of neuronal activity during hippocampal development produces a chronic focal epilepsy in the rat. *Journal of Neuroscience* **20**, 2904–2916.

Gambardella, A., Gotman, J., Cendes, F. & Andermann, F. (1995). Focal intermittent delta activity in patients with mesiotemporal atrophy: a reliable marker of the epileptogenic focus. *Epilepsia* **36**, 122–129.

Gibson, J. R., Beierlein, M. & Connors, B. W. (1999). Two networks of electrically coupled inhibitory neurons in neocortex. *Nature* **402**, 75–79.

Gomez-Di Cesare, C. M., Smith, K. L., Rice, F. L. & Swann, J. W. (1997). Axonal remodeling during postnatal maturation of CA3 hippocampal pyramidal neurons. *Journal of Comparative Neurology* **384**, 165–180.

Gulyás, A. I., Hajos, N. & Freund, T. F. (1996). Interneurons containing calretinin are specialized to control other interneurons in the rat hippocampus. *Journal of Neuroscience* **16**, 3397–3411.

Hájos, N. & Mody, I. (1997). Synaptic communication among hippocampal interneurons: properties of spontaneous IPSCs in morphologically identified cells. *Journal of Neuroscience* **17**, 8427–8442.

Hampson, R. E., Simeral, J. D. & Deadwyler, S. A. (1999). Distribution of spatial and nonspatial information in dorsal hippocampus. *Nature* **402**, 610–614.

Hormuzdi, S. G., Pais, I., Lebeau, F. E., Towers, S. K., Rozov, A., Buhl, E. H., Whittington, M. A. & Monyer, H. (2001). Impaired electrical signaling disrupts gamma frequency oscillations in connexin 36-deficient mice. *Neuron* **31**, 487–495.

Huerta, P. T. & Lisman, J. E. (1993). Heightened synaptic plasticity of hippocampal CA1 neurons during a cholinergically induced rhythmic state. *Nature* **364**, 723–725.

Huerta, P. T. & Lisman, J. E. (1996). Synaptic plasticity during the cholinergic γ-frequency oscillation *in vitro*. *Hippocampus* **6**, 58–61.

Ishizuka, N., Weber, J. & Amaral, D. G. (1990). Organization of intrahippocampal projections originating from CA3 pyramidal cells in the rat. *Journal of Comparative Neurology* **295**, 580–623.

Jefferys, J. G., Traub, R. D. & Whittington, M. A. (1996). Neuronal networks for induced '40 Hz' rhythms. *Trends in Neuroscience*s **19**, 202–208.

Khalilov, I., Esclapez, M., Medina, I., Aggoun, D., Lamsa, K., Leinekugel, X., Khazipov, R. & Ben-Ari, Y. (1997). A novel in vitro preparation: the intact hippocampal formation. *Neuron* **19**, 743–749.

Koch, C., & Segev, I. (1992). *Methods in Neuronal Modeling : from Synapses to Networks*. pp. 158–166. MIT Press, Cambridge, MA, USA .

Konopacki, J., Maciver, M. B., Bland, B. H. & Roth, S. H. (1987). Carbachol-induced EEG 'theta' activity in hippocampal brain slices. *Brain Research* **405**, 196–198.

Kudrimoti, H. S., Barnes, C. A. & Mcnaughton, B. L. (1999). Reactivation of hippocampal cell assemblies: effects of behavioral state, experience, and EEG dynamics. *Journal of Neuroscience* **19**, 4090–4101.

Lacaille, J. C., Mueller, A. L., Kunkel, D. D. & Schwartzkroin, P. A. (1987). Local circuit interactions between oriens/alveus interneurons and CA1 pyramidal cells in hippocampal slices: electrophysiology and morphology. *Journal of Neuroscience* **7**, 1979–1993.

Leinekugel, X., Medina, I., Khalilov, I., Ben-Ari, Y. & Khazipov, R. (1997). Ca^{2+} oscillations mediated by the synergistic excitatory actions of GABA(A) and NMDA receptors in the neonatal hippocampus. *Neuron* **18**, 243–255.

Leinekugel, X., Khalilov, I., Ben-Ari, Y. & Khazipov, R. (1998). Giant depolarizing potentials: the septal pole of the hippocampus paces the activity of the developing intact septohippocampal complex *in vitro*. *Journal of Neuroscience* **18**, 6349–6357.

Leung, L. W. (1985). Spectral analysis of hippocampal EEG in the freely moving rat: effects of centrally active drugs and relations to evoked potentials. *Electroencephalography and Clinical Neurophysiology* **60**, 65–77.

Leung, L. S. (1998). Generation of theta and gamma rhythms in the hippocampus. *Neuroscience and Biobehavioral Reviews* **22**, 275–90.

Levey, A. I., Edmunds, S. M., Koliatsos, V., Wiley, R. G. & Heilman, C. J. (1995). Expression of m1-m4 muscarinic acetylcholine receptor proteins in rat hippocampus and regulation by cholinergic innervation. *Journal of Neuroscience* **15**, 4077–4092.

Lewis, P. R. & Shute, C. C. (1967). The cholinergic limbic system: projections to hippocampal formation, medial cortex, nuclei of the ascending cholinergic reticular system, and the subfornical organ and supra-optic crest. *Brain* **90**, 521–540.

Li, X. G., Somogyi, P., Ylinen, A. & Buzsaki, G. (1994). The hippocampal CA3 network: an *in vivo* intracellular labeling study. *Journal of Comparative Neurology* **339**, 181–208.

Luk, W. P., Wu, C.P., Moldofsky, H. & L. Zhang. (2000). Adenosine modulation of intrinsic delta rhythms in the isolated whole hippocampus of mouse. *Sleep* 23 suppl., 95.

Lynch, G. & Schubert, P. (1980). The use of *in vitro* brain slices for multidisciplinary studies of synaptic function. *Annual Review of Neuroscience* **3**, 1–22.

McMahon, L. L., Williams, J. H. & Kauer, J. A. (1998). Functionally distinct groups of interneurons identified during rhythmic carbachol oscillations in hippocampus *in vitro*. *Journal of Neuroscience* **18**, 5640–5651.

MacVicar, B. A. & Tse, F. W. (1989). Local neuronal circuitry underlying cholinergic rhythmical slow activity in CA3 area of rat hippocampal slices. *Journal of Physiology* **417**, 197–212.

Madison, D. V., Lancaster, B. & Nicoll, R. A. (1987). Voltage clamp analysis of cholinergic action in the hippocampus. *Journal of Neuroscience* **7**, 733–741.

Martina, M., Vida, I. & Jonas, P. (2000). Distal initiation and active propagation of action potentials in interneuron dendrites. *Science* **287**, 295–300.

Michelson, H. B. & Wong, R. K. (1994). Synchronization of inhibitory neurones in the guinea-pig hippocampus i*n vitro*. *Journal of Physiology* **477**, 35–45.

Miles, R. & Wong, R. K. (1987). Inhibitory control of local excitatory circuits in the guinea-pig hippocampus. *Journal of Physiology* **388**, 611–629.

Miles, R., Traub, R. D. & Wong, R. K. (1988). Spread of synchronous firing in longitudinal slices from the CA3 region of the hippocampus. *Journal of Neurophysiology* **60**, 1481–1496.

Morris, M. (1995). Use of ion sensitive microelectrodes for recording intracellular ion levels. Measurement and manipulation of intracellular ions. *Methods in Neuroscience* **27**, 17–38.

Moser, M. B. & Moser, E. I. (1998). Distributed encoding and retrieval of spatial memory in the hippocampus. *Journal of Neuroscience* **18**, 7535–7542.

Mourre, C., Ben Ari, Y., Bernardi, H., Fosset, M. & Lazdunski, M. (1989). Antidiabetic sulfonylureas: localization of binding sites in the brain and effects on the hyperpolarization induced by anoxia in hippocampal slices. *Brain Research* **486**, 159–164.

Normand, M. M., Wszolek, Z. K. & Klass, D. W. (1995). Temporal intermittent rhythmic delta activity in electroencephalograms. *Journal of Clinical Neurophysiology* **12**, 280–284.

Oddie, S. D. & Bland, B. H. (1998). Hippocampal formation theta activity and movement selection. *Neuroscience and Biobehavioral Reviews* **22**, 221–231.

Ouanounou, A., Zhang, Y. & Zhang, L. (1999). Changes in the calcium dependence of glutamate transmission in the hippocampal CA1 region after brief hypoxia-hypoglycemia. *Journal of Neurophysiology* **82**, 1147–1155.

Parra, P., Gulyas, A. I. & Miles, R. (1998). How many subtypes of inhibitory cells in the hippocampus? *Neuron* **20**, 983–993.

Perez-Velazquez, J. L. & Zhang, L. (1994). *In vitro* hypoxia induces expression of the NR2C subunit of the NMDA receptor in rat cortex and hippocampus. *Journal of Neurochemistry* **63**, 1171–1173.

Pitler, T. A. & Alger, B. E. (1992). Cholinergic excitation of GABAergic interneurons in the rat hippocampal slice. *Journal of Physiology* **450**, 127–142.

Rhee, J. S., Ebihara, S. & Akaike, N. (1994). Gramicidin perforated patch-clamp technique reveals glycine-gated outward chloride current in dissociated nucleus solitarii neurons of the rat. *Journal of Neurophysiology* **72**, 1103–1108.

Sanchez-Vives, M. V. & McCormick, D. A. (2000). Cellular and network mechanisms of rhythmic recurrent activity in neocortex. *Nature Neuroscience* **3**, 1027–1034.

Saper, C. B. (1984). Organization of cerebral cortical afferent systems in the rat. II. Magnocellular basal nucleus. *Journal of Comparative Neurology* **222**, 313–342.

Scanziani, M., Capogna, M., Gahwiler, B. H. & Thompson, S. M. (1992). Presynaptic inhibition of miniature excitatory synaptic currents by baclofen and adenosine in the hippocampus. *Neuron* **9**, 919–927.

Schneiderman, J. H. (1986). Low concentrations of penicillin reveal rhythmic, synchronous synaptic potentials in hippocampal slice. *Brain Research* **398**, 231–241.

Schwartzkroin, P. A. & Knowles, W. D. (1984). Intracellular study of human epileptic cortex: in vitro maintenance of epileptiform activity? *Science* **223**, 709–712.

Schwartzkroin, P. A. & Haglund, M. M. (1986). Spontaneous rhythmic synchronous activity in epileptic human and normal monkey temporal lobe. *Epilepsia* **27**, 523–533.

Shen, H., Wu, C. & Zhang, L. (2000). Enhancement of glutamatergic synaptic responses by brief hypoxia-hypoglycemia in isolated whole mouse hippocampus *in-vitro*. *Society for Neuroscience Abstracts* **26**, 353.

Shinno, K., Zhang, L., Eubanks, J. H., Carlen, P. L. & Wallace, M. C. (1997). Transient ischemia induces an early decrease of synaptic transmission in CA1 neurons of rat hippocampus: electrophysiologic study in brain slices. *Journal of Cerebral Blood Flow and Metabolism* **17**, 955–966.

Shuttleworth, C. W. & Connor, J. A. (2001). Strain-dependent differences in calcium signaling predict excitotoxicity in murine hippocampal neurons. *Journal of Neuroscience* **21**, 4225–4236.

Skinner, F. K., Zhang, L., Velazquez, J. L. & Carlen, P. L. (1999). Bursting in inhibitory interneuronal networks: A role for gap-junctional coupling. *Journal of Neurophysiology* **81**, 1274–1283.

Skinner, F. K., Wu, C. & Zhang, L. (2001). Phase-coupled oscillator models can predict hippocampal inhibitory synaptic connections. *European Journal of Neuroscience* **13**, 2183–2194.

Spigelman, I., Zhang, L. & Carlen, P. L. (1992). Patch-clamp study of postnatal development of CA1 neurons in rat hippocampal slices: membrane excitability and K^+ currents. *Journal of Neurophysiology* **68**, 55–69.

Stumpf, C. (1965). Drug action on the electrical activity of the hippocampus. *International Review of Neurobiology* **8**, 77–138.

Tanabe, M., Gahwiler, B. H. & Gerber, U. (1998). Effects of transient oxygen-glucose deprivation on G-proteins and G-protein-coupled receptors in rat CA3 pyramidal cells *in vitro*. *European Journal of Neuroscience* **10**, 2037–2045.

Tesche, C. D. & Karhu, J. (2000). Theta oscillations index human hippocampal activation during a working memory task. *Proceedings of the National Academy of Sciences of the USA* **97**, 919–924.

Timofeev, I., Grenier, F., Bazhenov, M., Sejnowski, T. J. & Steriade, M. (2000). Origin of slow cortical oscillations in deafferented cortical slabs. *Cerebral Cortex* **10**, 1185–1199.

Traub, R. D., Miles, R. & Wong, R. K. (1989). Model of the origin of rhythmic population oscillations in the hippocampal slice. *Science* **243**, 1319–1325.

Traub, R. D. (1995). Model of synchronized population bursts in electrically coupled interneurons containing active dendritic conductances. *Journal of Computational Neuroscience* **2**, 283–289.

Tsuboi, M., Tanaka, Y. & Himori, N. (1994). Changes in mouse hippocampal EEG characteristics after oral administration of Ro 41-3696, nitrazepam, or zopiclone alone and in combination with ethanol. *Pharmacology* **49**, 278–285.

Vanderwolf, C. H. (1969). Hippocampal electrical activity and voluntary movement in the rat. *Electroencephalography and Clinical Neurophysiology* **26**, 407–418.

Verheugen, J. A., Fricker, D. & Miles, R. (1999). Noninvasive measurements of the membrane potential and GABAergic action in hippocampal interneurons. *Journal of Neuroscience* **19**, 2546–2555.

Vinogradova, O. S. (1995). Expression, control, and probable functional significance of the neuronal theta-rhythm. *Progress in Neurobiology* **45**, 523–583.

Voipio, J. & Kaila, K. (1994). Interstitial P_{CO_2} and pH in rat hippocampal slice measured by means of a novel fast CO_2/H^+ sensitive microelectrode based on PCV gelled membrane. *Pflügers Archiv* **423**, 193–201.

Wang, X. J. & Rinzel, J. (1992). Alternating and synchronous rhythms in reciprocally inhibitory model neurons. *Neural Computation* **4**, 84–97.

Whittington, M. A., Traub, R. D. & Jefferys, J. G. (1995). Synchronized oscillations in interneuron networks driven by metabotropic glutamate receptor activation. *Nature* **373**, 612–615.

Williams, J. H. & Kauer, J. A. (1997). Properties of carbachol-induced oscillatory activity in rat hippocampus. *Journal of Neurophysiology* **78**, 2631–2640.

Wilson, M. A. & Mcnaughton, B. L. (1994). Reactivation of hippocampal ensemble memories during sleep. *Science* **265**, 676–679.

Winson, J. (1978). Loss of hippocampal theta rhythm results in spatial memory deficit in the rat. *Science* **201**, 160–163.

Wu, C., Luk, W. & Zhang, L. (1999). Spontaneous GABAergic rhythms of intact hippocampus in vitro. *Society for Neuroscience Abstracts* **25**, 1497.

Xiong, Z. Q. & Stringer, J. L. (2000). Extracellular pH responses in CA1 and the dentate gyrus during electrical stimulation, seizure discharges, and spreading depression. *Journal of Neurophysiology* **83**, 3519–3524.

Zhang, L., Spigelman, I. & Carlen, P. L. (1991). Development of GABA-mediated, chloride-dependent inhibition in CA1 pyramidal neurones of immature rat hippocampal slices. *Journal of Physiology* **444**, 25–49.

Zhang, L. & Krnjevic, K. (1993). Whole-cell recording of anoxic effects on hippocampal neurons in slices. *Journal of Neurophysiology* **69**, 118–127.

Zhang, L., Weiner, J., Valiante, T. A., Velumian, A. A., Walson, P., Jahromi, S. S., Schetzer, S. & Carlen, P. L. (1994). Effects of internally applied anions on the $Ca2^{+}$ activated afterhyperpolarization in rat hippocampal neurons. *Pflügers Archiv* **426**, 247–253.

Zhang, L., Han, D. & Carlen, P. L. (1996). Temporal specificity of muscarinic synaptic modulation of the Ca^{2+}-dependent K^{+} current (I_{sAHP}) in rat hippocampal neurones. *Journal of Physiology* **496**, 395–405.

Zhang, Y., Perez Velazquez, J. L., Tian, G. F., Wu, C. P., Skinner, F. K., Carlen, P. L. & Zhang, L. (1998). Slow oscillations ($\leqslant$ 1 Hz) mediated by GABAergic interneuronal networks in rat hippocampus. *Journal of Neuroscience* **18**, 9256–9268.

Acknowledgements

This work was supported by a research grant to L. Zhang from the Canadian Institutes of Health Research (CIHR, MOP-44092). W. P. Luk is a recipient of the NSERC and Ontario Graduate Scholarships. The authors thank Drs L. S. Leung and F. Skinner for their valuable discussion and Drs F. Amzica and M. Morris for their help in establishing ion-sensitive electrodes.